EFFECT OF MATRIX COMPOSITION ON THE UNIAXIAL TENSILE BEHAVIOR OF CARBON TEXTILE REINFORCED CEMENTITIOUS COMPOSITES

A THESIS SUBMITTED TO
THE GRADUATE SCHOOL OF NATURAL AND APPLIED SCIENCES
OF
MIDDLE EAST TECHNICAL UNIVERSITY

BY

M. HAMAHANG SHERZAI

IN PARTIAL FULFILLMENT OF THE REQUIREMENTS
FOR
THE DEGREE OF MASTER OF SCIENCE
IN
CIVIL ENGINEERING

DECEMBER 2023

Approval of the thesis:

EFFECT OF MATRIX COMPOSITION ON THE
UNIAXIAL TENSILE BEHAVIOR OF
CARBON TEXTILE REINFORCED CEMENTITIOUS COMPOSITES

submitted by **M. Hamahang Sherzai** in partial fulfillment of the requirements for the degree of **Master of Science** i**n Civil Engineering, Middle East Technical University** by,

Prof. Dr. Halil Kalıpçılar
Dean, **Graduate School of Natural and Applied Sciences** _____

Prof. Dr. Erdem Canbay
Head of the Department, **Civil Engineering** _____

Prof. Dr. İsmail Özgür Yaman
Supervisor, **Civil Engineering, METU** _____

Examining Committee Members:

Prof. Dr. Sinan Turhan Erdoğan
Civil Engineering, METU _____

Prof. Dr. İsmail Özgür Yaman
Civil Engineering, METU _____

Assoc. Prof. Dr. Serdar Göktepe
Civil Engineering, METU _____

Assoc. Prof. Dr. Çağla Meral Akgül
Civil Engineering, METU _____

Asst. Prof. Dr. Emin Şengün
Civil Engineering, Ankara Yıldırım Beyazıt University _____

Date: 07.12.2023

I hereby declare that all information in this document has been obtained and presented in accordance with academic rules and ethical conduct. I also declare that, as required by these rules and conduct, I have fully cited and referenced all material and results that are not original to this work.

Name Last name: M. Hamahang Sherzai:

Signature:

ABSTRACT

EFFECT OF MATRIX COMPOSITION ON THE
UNIAXIAL TENSILE BEHAVIOR OF
CARBON TEXTILE REINFORCED CEMENTITIOUS COMPOSITES

M. Hamahang Sherzai
Master of Science, Civil Engineering
Supervisor: Prof. Dr. İsmail Özgür Yaman
December 2023, 108 pages

Textile-reinforced concrete (TRC) is a distinct type of concrete that employs continuously manufactured textiles instead of traditional steel reinforcing bars to manage tensile stresses within a structure. As with any composite material, the mechanical properties of composites are primarily determined by the proportions and properties of the individual materials that make up the composite. Consequently, the mechanical properties of TRC are expected to be influenced by both the amounts and fibers

of the textile and the surrounding cementitious matrix. In addition, the adhesion between the textile and the cementitious matrix, as well as any interlocking mechanism introduced during the textile manufacturing process, could also play a significant role. It should be noted that in textile nomenclature, yarns or threads are initially formed from bundles of continuous fibers also called monofilaments. Later, textiles can be produced by various manufacturing techniques using a variety of geometric patterns. Weaving is one of those manufacturing technique in which two distinct sets of yarns or threads are interlaced at right angles to form the textile. The yarns along the textile length are termed warp yarns, and those along its width are termed as weft yarns.

In this experimental study, carbon textiles woven in a grid-like pattern are used to produce the C-TRCC specimens. In addition, unlike the usual use of these textiles in the warp direction, the textiles were used in the weft direction. As for the cementitious matrix, two different base matrices (M7 and ECC) with different binder contents were used. These two base matrices incorporated different types (steel and PVA) and amounts (1% and 2%) of discrete short fibers. Uniaxial tensile tests are performed on C-TRCC specimens prepared using carbon textiles with different reinforcement ratios.

As a result of more than 70 C-TRCC specimens, it was observed that carbon textiles experienced a slippage-like phenomenon in which the core filaments within the yarn slipped from the sheath filaments adhering to the cementitious matrix. It was also observed that the stiffer M7 matrix exhibited more brittle behavior compared to the softer ECC matrix.

Keywords: Carbon textile reinforced concrete, reinforcement ratio, weft direction, matrix toughness, slippage

ÖZ

KARBON TEKSTİL TAKVİYELİ ÇİMENTOLU KOMPOZİTLERİN TEK EKSENLİ ÇEKME DAVRANIŞINA MATRİS BİLEŞİMİNİN ETKİSİ

Sherzai, M. Hamahang
Yüksek Lisans, İnşaat Mühendisliği
Tez Yöneticisi: Prof. Dr. İsmail Özgür Yaman
Aralık 2023, 108 sayfa

Tekstil takviyeli beton (TRC), bir yapıdaki gerilmeleri karşılayabilmek için geleneksel çelik donatılar yerine tekstillerin kullanıldığı farklı bir beton türüdür. Herhangi bir kompozit malzemede olduğu gibi, kompozitlerin mekanik özellikleri öncelikle kompoziti oluşturan bileşenlerinin oranları ve özellikleri tarafından belirlenir. Dolayısıyla, TRC'nin mekanik özelliklerinin hem tekstilin hem de onu çevreleyen çimentolu matrisin miktar ve özelliklerinden etkilenmesi beklenmektedir. Buna ek olarak, tekstil ve çimentolu matris arasındaki bağ ve tekstil üretim süreci nedeniyle ortaya çıkan herhangi bir kenetlenme mekanizması da önemli bir rol oynayabilir. Tekstil terminolojisinde, ipliklerin veya ipliklerin başlangıçta monofilamentler olarak da adlandırılan sürekli elyaf demetlerinden oluştuğu unutulmamalıdır. Daha sonra, tekstiller çeşitli geometrik desenler kullanılarak çeşitli üretim teknikleri ile üretilebilir. Dokuma, tekstili oluşturmak için iki farklı iplik veya iplik setinin dik açılarla birbirine geçtiği bu üretim tekniklerinden biridir. Tekstil uzunluğu boyunca uzanan iplikler çözgü iplikleri olarak adlandırılırken, genişliği boyunca uzanan iplikler atkı iplikleri olarak adlandırılır.

Bu deneysel çalışmada, C-TRCC numunelerini üretmek için ızgara benzeri bir desende dokunan karbon tekstiller kullanılmıştır. Ayrıca, bu tekstillerin çözgü yönündeki alışılagelmiş kullanımından farklı olarak, tekstiller atkı yönünde kullanılmıştır. Çimentolu matris olarak, farklı bağlayıcı içeriklerine sahip iki farklı temel matris

(M7 ve ECC) kullanılmıştır. Bu iki temel matris, farklı tiplerde (çelik ve PVA) ve miktarlarda (%1 ve %2) ayrık kısa lifler içermektedir. Karbon tekstiller farklı donatı oranlarında kullanılmış ve hazırlanan C-TRCC numuneleri üzerinde tek eksenli çekme testleri gerçekleştirilmiştir.

Test edilen 70 adet C-TRCC numunesi sonucunda, karbon tekstillerin, iplik içerisindeki çekirdek filamentlerin çimentolu matrise yapışan kılıf filamentlerinden kaydığı kayma benzeri bir fenomen yaşadığı gözlemlenmiştir. Ayrıca, daha sert olan M7 matrisinin daha yumuşak olan ECC matrisine kıyasla daha kırılgan bir davranış sergilediği de gözlemlenmiştir.

Anahtar Kelimeler: Karbon tekstil donatılı beton, donatı oranı, atkı yönü, matris tokluğu, kayma olayı

To my beloved family,

ACKNOWLEDGMENTS

First and foremost, I would like to express my sincere gratitude to my supervisor Prof. Dr. İsmail Özgür Yaman for his continuous support, perfect guidance, and insight throughout the study.

I could not have undertaken this journey without Iraj Sharifi. I am thankful for his invaluable support in every step of the preparation of my thesis. Above all, the experimental procedure of the thesis was completed with him.

This work is funded by the Scientific and Technological Research Council of Turkey under grant number TUBİTAK 121N240. I appreciate the in-kind support provided by Fibrobeton, Baştaş Çimento, Master Builders Solutions, and Solidian companies.

And last but not least, I would like to thank my family for their endless love, encouragement, and patience no matter what path I choose throughout my whole life

TABLE OF CONTENTS

LIST OF TABLES

LIST OF FIGURES

LIST OF ABBREVIATIONS

TRCC	: Textile Reinforced Cementitious Composites
TRC	: Textile Reinforced Concrete
ECC	: Engineered Cementitious Composites
DIC	: Digital Image Correlation
C-TRCC	: Carbon Textile Reinforced Cementitious Composites
TRM	: Textile Reinforced Mortar

LIST OF SYMBOLS

σ_{cr} : First crack strength

σ_u : Ultimate strength

ρ : Reinforcement ratio

t : Thickness

σ_t : Maximum stress on carbon textile

E_f : Cracked modulus of elasticity

CHAPTER 1

INTRODUCTION

1.1. General

Conventional concrete is the world's most widely used building material due to its technical advantages as well as availability, versatility and low cost. However, it has some limitations, such as low tensile strength and susceptibility to cracking. To overcome such limitations, conventional concrete is often reinforced with steel bars and sometimes with fibers.

Textile reinforced concrete (TRC) is a special type of concrete in which a fine-grained cementitious matrix is reinforced this time by continuous fibers. The history of TRC dates back to the mid-19th century, when Joseph Monier discovered a method of reinforcing concrete with wire mesh. Today, textiles of different materials such as glass, carbon, basalt and aramid are used in TRC applications. These textiles provide greater strength and durability than steel, besides allowing greater design flexibility and less weight. Non-metallic textiles or fabrics are used at a certain amount, to avoid the brittle nature of the cementitious matrix and to achieve a pseudo-ductile mechanical behaviour (Venigalla et al., 2022).

For TRC applications, two-dimensional (2D) or three-dimensional(3D) textiles made from multifilament yarns are usually used. These yarns, which have a range of geometric variations such as crimped or straight, are industrially manufactured using weaving, knitting and spinning techniques. These textiles are manufactured according to the intended use of the TRC.

The weaving process, which takes place in a stationary machine called a loom, is one of the manufacturing techniques in which two different sets of yarns or threads are interlaced at right angles (0° / 90°) to form the textile. The yarns along the length of the textile are called the warp yarns and those along the width are called the weft yarns. In other words, the warp thread, also known as the longitudinal thread, runs

vertically (0°) on the loom from the bottom to the top of the textile. These threads are usually stationary and attached to the loom frame. They provide the basic structure of the fabric and are kept taut during the weaving process. On the other hand, the weft threads, also known as horizontal or crosswise threads, run horizontally (90°) across the textile, interlacing with the warp threads. These threads are inserted over and under the warp threads using a shuttle or other weaving tools. The weft threads are the ones that create the patterns and design of the textile.

Besides the textiles, TRC uses Portland cement and supplementary cementitious materials as the binder phase, mixed with fine aggregates to achieve a more homogeneous matrix. Superplasticisers are also used to increase the strength of the matrix and to obtain a workable mix. In the literature, it is the so-called M-7 mixture which is often used in TRC applications (Esmaeili et al., 2017; Lieboldt & Mechtcherine, 2013). Recently, researchers have started to incorporate randomly distributed short fibers into the matrix. This is a relatively new feature and an important aspect for improving the performance and the properties of the TRC.

It is anticipated that the mechanical properties of TRC will be influenced by both the amount and properties of the textile and the surrounding cementitious matrix. In addition, the adhesion between the textile and the cementitious matrix, as well as any interlocking mechanism introduced during the textile manufacturing process, could also play a significant role. A review of the literature shows that the mechanical properties of TRC specimens are mostly determined in the warp direction, and there is limited information on the behaviour of TRC specimens in the weft direction (Mattarollo et al., 2023; Rampini et al., 2019). Moreover, the leno weave is a specific type of woven structure in which two warps yarns are twisted around the weft yarns, creating a stronger interlock and resulting in a durable textile with an openwork structure (Peled et al., 2017) has seldomly being studied. Finally, the use of short fibers to improve the matrix properties is also a relatively new subject (Barhum & Mechtcherine, 2012; M. Zhang & Deng, 2022).

1.2. Objective and scope

In this thesis, the mechanical behaviour of TRC specimens utilizing the weft direction of the carbon textile as the reinforcement together with an improved cementitious matrix toughness will be explored. With this in mind, the aim of this study is to determine the effect of cementitious matrix ductility and the reinforcement ratio on the uniaxial tensile behaviour of carbon textile reinforced cementitious composites (C-TRCC). This is done by using carbon textiles at different reinforcement ratios in two different cementitious matrices with different binder types and amounts. The first matrix is commonly used in TRC applications and is known as the M7 matrix. In addition, a relatively softer matrix incorporating a significant amount of fly ash is also used, which is derived from the conventional M45 mix of ECC. Later, fibers (steel and PVA) are also added to both matrices to increase the ductility of the matrices, and the uniaxial tensile behavior of carbon textiles is determined when used with cementitious matrices of different properties.

There are five chapters in this thesis, including this one. The second chapter presents a brief literature review of textile reinforced concrete, textile types, history of fibers, together with the widespread common tests and research in this field. The third chapter describes the experimental study and the properties of the material used, together with a detailed explanation of the experimental work. The fourth chapter contains the general test results along with the discussion and comments on them. In the last chapter, the recommendations and conclusions for future studies are listed. Moreover, the test results of each test specimen are presented in the appendices.

CHAPTER 2

LITERATURE REVIEW

2.1. Historical use of fibers

Besides having many advantages, concrete is a brittle material, because of its low tensile strength (approximately 10% of its compressive strength) and its low post-crack performance (Lee et al., 2016). In order to increase the tensile performance of concrete, steel reinforcement is often needed.

Across various civilizations and time periods, different fibers types have also been integrated into concrete to enhance its performance and durability. For instance, the Roman Empire was famous for its advanced construction techniques, including the the usage of fibers in concrete. They used materials such as horsehair, straw, and vegetable fibers in their concrete structures to build baths and domes. These fibers assisted to improve the concrete's tensile strength and control cracking.

In the 19th century, the industrial revolution led to the development of new types of fibers for concrete reinforcement. For example, iron wires and rods were embedded in concrete to increase its strength and resistance to tension. This laid the foundation for modern reinforced concrete.

In the 20th century, synthetic fibers began to be used in concrete. Asbestos fibers were widely used as reinforcement due to their excellent fire resistance and strength. Nonetheless, their usage decreased because of health concerns associated with asbestos exposure. Various synthetic fibers, including nylon, polyproplene, and polyster have been employed to improve the properties of concrete such as resistance to crack and impact resistance.

Today, fiber reinforced concrete (FRC) is widely used in various types of construction projects. These fibers are normally incorporated in small quantities and evenly distributed throughout the concrete matrix. These fibers offer higher tensile strength,

durability and resistance to corrosion. Hence, it makes them appropriate for different applications such as tunnels, architectural elements and bridges.

The historical use of fibers in concrete reveals the long-standing recognition of the benefits of reinforcement in enhancing the performance and longevity of concrete structures. Advances in fiber technology has led to the development of new materials and methods, expanding the possibilities for reinforced concrete in modern construction.

2.2. Development of TRC

Textile-reinforced concrete (TRC) is a composite material that combines a cement-based matrix with high-performance embedded textile reinforcements, which are continuous multifilament yarns made of carbon, alkali-resistant glass, or polymers. TRC is a relatively new development in the field of materials of construction and offers several advantages compared to traditional reinforced concrete.

The main benefits of TRC are its high tensile strength and pseudo-ductile behavior, quantified through large deformations because of its achievement in multiple cracking (Barhum & Mechtcherine, 210). Consequently, this material can be counted as a suitable material for construction applications not only for strengthening or repair of old structural elements but also for new structures that are made of reinforced concrete or other conventional materials (Naaman, 2010).

Even though the concept of using textiles as reinforcement was explored as early as the 19th century, the modern era of TRC started in the 1990s by the introduction of modern textiles. In this era, the usage of textile materials, such as glass and carbon fibers gained its reputation as an alternative to traditional steel reinforcement. Scientists and engineers began to investigate the possibility of using textile reinforcement to improve the durability of concrete structures. Later, in the early 2000s, a lot of research and development efforts were undertaken to achieve a comprehensive insight into the behaviour of TRC(Williams Portal et al., 2015; Yao et al., 2016).

For example, Germany set up the guideline Textile Reinforced Concrete in 2001(Mechtcherine, 2016). This guideline provided recommendations for the design, production, and application of TRC. After that, different organizations and institutions carried out studies on different textile materials, techniques, and mechanical properties of TRC(Peled et al., 2017). By time, the understanding and acceptance of TRC improved, and its applications grew to different structural as well as architectural elements, especially in the restoration and strengthening of historical structures (Holčapek et al., 2017).

2.3. Applications of TRC

TRC is often used for improving the load-bearing capacity and durability of structures due to its excellent flexibility and high tensile strength, qualities that make it suitable for building complex shapes and facilitating lightweight construction solutions (Fibre & Engineering,PP.234). Therefore, TRC is used in a wide variety of applications. Its adaptability allows it to be used in architectural components such as cladding panels, slender structures and facades. In addition, TRC is invaluable in strengthening new structures and restoration of existing buildings, such as bridges and historical structures, as well as in precast concrete, tunnel linings, geotechnical engineering, etc.

Because of its ductile behavior and energy absorption capacities, TRC can also be utilized in applications that need impact resistance. For instance, it can be applied to blast-resistant structures, protective barriers or structures exposed to dynamic loads(Weber & Mechtcherine, 2016).

It has also been used in geotechnical applications. For example, with its improved durability and crack resistance, TRC can be used for tunnel lining(Liu et al., 2016). Its lightweight nature makes it easier to control and install, thus reducing construction time and cost(Cibulka et al., 2019). Further, it can be applied to soil and slope stabilization, as well as in the reinforcement of retaining walls. It can enhance the soil's bearing capacity and provide stability for the structures(Abid & Rathod, 2022).

Moreover, TRC is compatible with the principles of sustainable construction because of its lower carbon footprint than traditional reinforced concrete. The usage of textile reinforcement decreases the consumption of steel which results in reduced energy consumption and CO_2 emissions during production (Portal et al., 2014). At the end, the versatility and improved performance characteristics of TRC makes it an amazing choice in different construction and engineering applications.

2.4. Production Techniques of Textiles

The production of textiles used in TRC involves several techniques to manufacture the textile reinforcements. Some of the key production techniques used for TRC textiles are summarized in this section.

2.4.1. Weaving

Weaving is one of the most common techniques for producing textile reinforcements for TRC. The process of interlacing two sets of yarn (Warp and Weft) to create a textile can be performed on various types of looms, which are devices that produce textiles (Triantafillou, 2016). The weaving pattern specifies the structure and design of the fabric as shown in Figure 2-1. The leno weave is a specific type of woven structure in which two warps yarns are twisted around the weft yarns, creating a stronger interlock and resulting in a durable textile with an openwork structure (Peled et al., 2017).

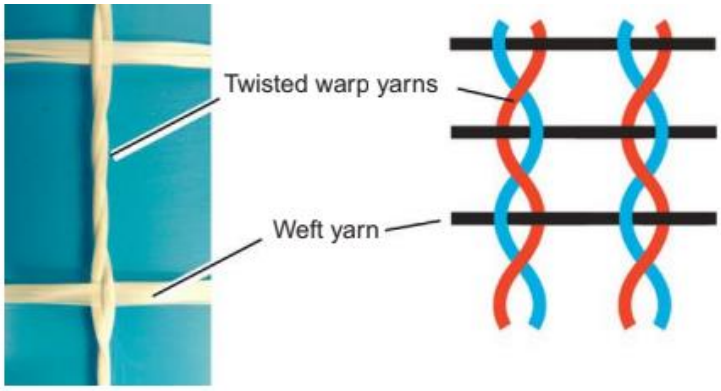

Figure 2-1 A leno weave with glass weft yarns(left) schematic diagram of a leno (Textile Fibre & Engineering, PP.10.)

2.4.2. Knitting

Knitting is another technique used to create textile reinforcements for TRC. Knitted fabrics are produced by interlocking loops of yarn with specialized knitting machines. Knitted fabrics are often more flexible and can conform to complex shapes, making them suitable for applications that require flexibility, such as curved surfaces (Spencer, 1989).

2.4.3. Non-woven

Non-woven fabrics can be created through bond of fibers together by mechanical, thermal or chemical processes, rather than knitting and weaving. These non-woven fabrics are commonly used in disposable products such as geotextiles and filtration media (Peled et al., 2017)

2.4.4. Spinning

Spinning is a process of changing fibers into yarns. This method involve twisting or spinning the fibers together to make continuous strands of yarn that can be further processed into fabric (Tiedemann & Jakes, 2006).

2.5. Textiles used in TRC Applications

There are several types of textiles such as carbon, AR-glass, basalt and aramid, which will be explained in the proceeding subsections.

2.5.1. AR-Glass Textile

AR-Glass textile refers to a type of textile material that is made from alkali-resistant glass fibers, and they are traditionally used as reinforcement in fiber-reinforcement concrete (FRC) or fiber-reinforced polymer composites. It is a special composition of glass that shows excellent resistance to alkaline substances, such as those found in cementitious materials like concrete. Glass fibers are produced to withstand the highly alkaline environment present in concrete and making them suitable for reinforcement purposes.

AR-Glass fibers are typically woven or non-woven into a fabric-like structure, which can then be embedded in concrete or combined with a polymer matrix to create a composite material. The alkali resistance of AR-Glass fibers ensures that they do not degrade or weaken when exposed to the alkaline conditions present in concrete. This resistance is of paramount importance because glass fibers, such as those used in fiberglass, can be susceptible to a chemical reaction known as alkali-silica reaction (ASR) when exposed to alkaline environments. ASR has the potential to cause cracking and deterioration of concrete structures, compromising their structural integrity and longevity. AR-Glass fibers prevent this reaction from occurring, ensuring the long-term performance of TRC.

AR-Glass textiles are known for their lightweight nature, non-combustible properties, and excellent dimensional stability. Therefore, they are used in various construction applications, including precast concrete elements, thin-walled structures, tunnel linings, bridge decks and repair and retrofitting of existing structures.

2.5.2. Carbon Textile

Carbon textiles are a special type of textile material made from carbon fibers. Carbon fiber atoms are arranged in a crystalline structure, resulting in remarkable strength, stiffness and lightness. These fibers are produced by knitting or weaving into a fabric like form, creating a flexible and versatile material. Carbon fibers show an excellent resistance to different chemicals such as acids, alkalis, and organic solvents. This resistance makes carbon textiles appropriate for applications in corrosive environments or chemical processing industries. Besides, carbon fibers have high thermal conductivity, permitting effective heat dissipation. Carbon textiles find applications in thermal management systems, such as in heat shields, protective clothing, and composite materials used in high temperature environments (Mansur de Castro Silva & de Andrade Silva, 2020). Additionally, carbon textiles show excellent dimensional stability, meaning they have minimal expansion or contraction under changes in temperature and humidity. Because of this property, carbon textiles are suitable for applications where precise dimensional control is needed, such as composite manufacturing. Due to all the above-mentioned properties, carbon textiles are used in different industrial sectors and applications such as Aerospace and defense, sport and recreation and repair and retrofitting of civil engineering structures.

Carbon textile reinforced concrete (CTRC) is a kind of composite material that adds carbon textile reinforcements with a concrete matrix to make a lightweight and high-strength structural material (Mansur de Castro Silva & de Andrade Silva, 2020). Hence, CTRC is greatly recommended for repairing and retrofitting of structures. Owing to the non-corrosive property of textiles, it is highly recommended to substitute reinforced concrete that faces corrosion substances while in service.

In practice, reinforcement ratio in CTRC is chosen to provide an adequate tensile strength to counteract the tensile stresses developed in concrete matrix. Commonly higher reinforcement ratio results in increased tensile strength, control of cracks and higher flexural strength in CTRC elements. Nonetheless, the reinforcement ratio

needs to be balanced with other factors, like durability, cost considerations and constructability.

It is crucial to note that the reinforcement ratio alone cannot specify the performance of carbon textile reinforced concrete. But the properties of carbon textile reinforcement and the quality. For example, the type of carbon fiber, the arrangement of fibers and bonding characteristics, can also influence the mechanical behavior and efficiency of the reinforcement in CTRC.

2.5.3. Basalt Textile

Basalt textile refers to a type of textile material made from basalt fibers. Most basalt fibers are obtained from the natural volcanic rock known as basalt. This type of rock is melted at high temperatures and then extruded through fine nozzles to form fibers. These fibers are knitted or woven into a fabric-like structure to create basalt textiles. This type of textile offers plenty of advantages because of the properties of basalt fibers (Du et al., 2017). It has high resistance to temperature and high strength. It is also resistant to chemicals.

2.6. Mechanical Behavior of TRC

Research showed that TRC exhibits higher tensile strength that is typically reached at relatively large formations (D. Jesse & Jesse, 2009). These large deformations are crucial before failure of material and taking into account the safety of structure as well as releasing of energy in case of impact loading. Textile reinforcements distribute the tensile stresses more uniformly throughout the material, limiting the width of cracks. This results in enhanced durability and structural performance, particularly in applications where cracking can lead to degradation or failure. Besides, the use of textile reinforcements in TRC reduces the weight of the material compared to traditional steel reinforcement. This not only makes TRC easier to handle and transport but also enables the production of thinner and lighter concrete elements. As a result,

TRC can contribute to the development of more sustainable and resource-efficient structures.

The mechanical behavior of TRC can be influenced by various factors, including the properties of the textiles, the cementitious matrix, and the interaction between them. Several aspects of TRC mechanical properties is explained below.

2.6.1. Tensile Behavior

Many researchers have investigated the uniaxial tensile behavior of TRC (Contamine et al., 2011,Santis et al., 2017,Dong et al., 2020, Deng et al., 2020). The uniaxial tensile test of a TRC specimen is performed in a loading frame under the load and displacement control gauges, and the recording can be measured by a load cell. The lack of standards is a challenge that prevents designers, manufacturers, and contractors from fully applying the uniaxial tensile test. Therefore, they use the recommendations for installation, design, and control of the tests (Santis et al., 2017).

For example, European countries have some recommendations for testing TRC composites. For example, RILEM 232-TDT has described a recommendation for the uniaxial tensile test of TRC to specify the load-deformation of tensile specimens (RILEM TC 232-TDT (Wolfgang Brameshuber) et al., 2016). Figure 2-2 represents a typical behavior of textile reinforced concrete when subjected to the uniaxial tensile stresses. The behavior of the TRC can be divided into three regions (F. Jesse, 2015). The first region (I) reveals the free crack condition. In this region, TRC shows a relatively linear-elastic behavior to the point where the enlargement in the stress makes the formation of the first macro-crack due to the stiffness of the mortar matrix and fibers. The second region (IIa) is the state of crack formation. This state describes the quasi-ductile behavior in the TRC. The creation of multiple cracks in this portion of the curve appears because of the increased stiffness in the post-matrix area released by the fibers that crosscut the matrix crack (Hartig et al., 2008). The crack widening stage (IIb) forms the final region. In this stage, few cracks could appear, or none of the cracks might occur. However, the cracks that happened before get wider

and wider until the tensile strength of the multifilament yarn of TRC appears. Thus, failure occurs. In the stages explained above, the formations of the cracks on the outer surface of the specimens can be witnessed through the naked eyes while applying the uniaxial tensile load.

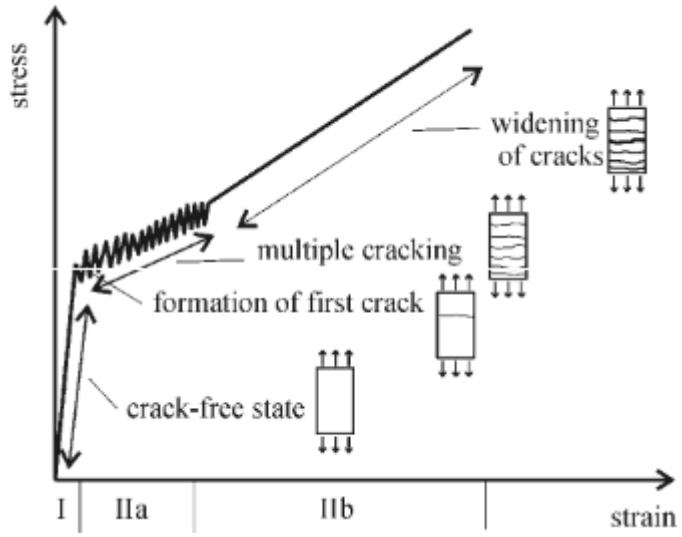

Figure 2-2 TRC specimen subjected to uniaxial loading and the states of cracks (Barhum & Mechtcherine, 2010)

2.6.2. Flexural Behavior

TRC has improved flexural performance compared to traditional concrete due to the textile reinforcement. These fabrics distribute and carry the applied bending loads, resulting in high flexural strength and stiffness. TRC can resist to prevent higher deformations and show improved load bearing capacity. (Brückner et al., 2006, Williams Portal et al., 2017).

2.6.3. Shear Behavior

The textile reinforcement can contribute to the shear resistance and reduce the possibility of shear failure in concrete elements subjected to lateral forces. Therefore, the shear behavior of TRC is influenced by the textile reinforcements and the matrix.

The effectiveness of textile reinforcement depends on several factors, such as fiber arrangement, bonding characteristics, and fiber type (Brückner et al., 2006).

2.6.4. Bond Behavior

The bond between the fabrics and the matrix material is critical for the overall performance of TRC(Yan et al., 2023). An adequate amount of bond is necessary to make sure load transfer between textile reinforcement and the matrix. There are some factors that affect the bond such as fiber surface treatment, fiber/matrix interface properties, and compaction while production of elements of TRC (Saidi et al., 2022).

2.6.5. Durability and Aging

TRC mechanical behavior can also be influenced by long-term exposure to environmental factors, such as changes in temperature, chemical attacks, and moisture. Thus, a proper selection of materials and consideration for design is important to make sure the durability of TRC structures by passage of time. Additionally, the impact of TRC under creep , shrinkage need to be also taken into account in structural design (Alma & Ghiassi, 2021; Yan et al., 2023).

All the aforementioned behaviors led us to a conclusion that the mechanical behavior of TRC can vary depending on the special materials used, fabrication techniques, and design considerations. For this, sometimes experimental and analytical models are often used, to study and predict the mechanical behavior of TRC structures under different environmental states and loadings.

2.6.6. Effects of Reinforcement Ratio

In TRC, the reinforcement ratio is defined as the ratio of the area or volume of textile reinforcement to the total area or volume of the concrete matrix.

$$\rho = \frac{As}{b * d}$$

ρ reinforcement ratio, b the cross-sectional width of the matrix, d is the thickness of the matrix,

It plays a vital role in determining the mechanical behavior and performance of TRC structures. For example, it can result in high tensile strength and control of cracks. By increasing the reinforcement ratio, there is a higher amount of textile reinforcement to carry tensile loads and control cracking. Thus, it can result in improved crack control and increased resistance to cracking in structural elements of TRC. Moreover, reinforcement ratio decrease cracks width but the number of small crack increase because fabric can rapidly contribute to tensile stress acting on the concrete matrix (Yang et al., 2023). Having a higher reinforcement ratio in TRC contributes to increased flexural strength and stiffness. It can help to distribute and carry bending loads and enhance the whole load-carrying capacity of the composites. This is especially important in applications where higher flexural strength is needed, such as slab and beams.

Furthermore, TRC with higher reinforcement ratios tends to show higher ductility and energy absorption capacity. This is because the increased amount of textile reinforcement permits for more deformations and dissipation of energy prior to failure occurring. This can be more important in buildings subjected to impact loads or dynamic loads.

However, it also makes them more expensive to build because we need to use more materials. Thus, it is really important to utilize the right amount of reinforcement ratio in utilizing TRC.

2.6.7. Effects of Matrix Properties

Different matrix compositions have been developed for the production of TRC by considering the requirements of workability, durability and sufficient bonding to the textile reinforcement. In most cases, the fine-grained concrete used for the

production of TRC has a water/binder ratio of 0.3-0.4 by volume of 40-50% (Textile Fibre Composite in Civil Engineering, Page.27-28)

In addition, a high binder content is necessary for adequate bonding between the fine concrete and the filaments of the textile reinforcement and for the workability of the fresh concrete. The maximum aggregate size depends on the spacing between the yarns of the textile reinforcement layers and the size of the meshes. The maximum aggregate grain sizes range between 1 and 2 mm(Mechtcherine, 2013).

There are five types of fine-grained matrix compositions as developed and utilized for TRC with Collaborative Research Center 528 at TU Dresden such as M1,M3, M7,PZ-0899-01 and FA-1200-01(Textile Fibre Composites in Civil Engineering. Page. 27-28.) as can be shown in Figure 2-3.

Concrete needs to have a relatively high form stability after casting and higher adhesion to the substrate in order to be sprayed on incline and vertical surfaces or applied overhead for repair and reinforcement. These requirements can be met with M1, M3 and M7 matrices. The properties for hardened concrete for TRC specimens can be found in Figure 2-4.

Materials		Mineral-based matrices				
		PZ-0899-01 SFB 532	FA-1200-01 SFB 532	M1 SFB 528	M3 SFB 528	M7 SFB 528
Cement c	kg/m^3	490	210	539	549	839
Cement type	–	CEM I 52.5	CEM I 52.5	CEM III/B 32.5	CEM I 32.5 R	CEM I 32.5 R
Fly ash f	kg/m^3	175	455	243	246	–
Silica fume s		35	35	–	–	–
Silica slurry (w:s = 1:1)		–	–	53.9	54.6	–
Binder (c+f+s)		700	700	809	822	839
Plasticizer	% by mass of binder	1.0–1.5	0.9	2.1–2.2	2.3–2.4	2.1–2.2
Siliceous fines 0–0.125 mm	kg/m^3	500	470	–	–	–
Siliceous fine sand 0.2–0.6 mm		715	670	–	–	–
Sand 0–1 mm		–	–	1079	1092	1189
Water		280	280	242.7	245.6	279.7
w/c	–	0.57	1.33	0.45	0.45	0.33
w/b = w/(c+f+s)	–	0.40	0.40	0.30	0.30	0.33

Figure 2-3 Composition of various TRC matrices (Textile Fibre & Engineering Composite, P30)

Materials		Mineral-based matrices				
		PZ-0899-01 SFB 532	FA-1200-01 SFB 532	M1 SFB 528	M3 SFB 528	M7 SFB 528
Compressive strength 28d	MPa	74.0	32.0	53.7	63.5	72.3
Flexural strength 28d	MPa	7.6	5.1	7.5	8.6	11.2
Young's modulus 28d	GPa	33.0	24.8	21.0	25.5	30.8
Shrinkage 28d	mm/m	0.81	0.56	0.2	0.83	0.53
Shrinkage 360d	mm/m	1.01	–	0.85	1.27	–

Figure 2-4 Properties of hardened TRC matrices (Textile Fibre Composite Civil & Engineering, P.31)

In recent years, as a result of the studies at the University of Michigan, a high-performance fiber-reinforced composite material with a patent name of "Engineered Cementitious Composites (ECC)" has been developed. Depending on the composition, the properties of ECC may change and compressive strengths within the range of 30-100MPa have been reported. Nonetheless, this composite material has a very high tensile strain capacity (within the range of 3-5%). The crack width is typically below <100μm during strain-hardening(Şahmaran et al., 2009).

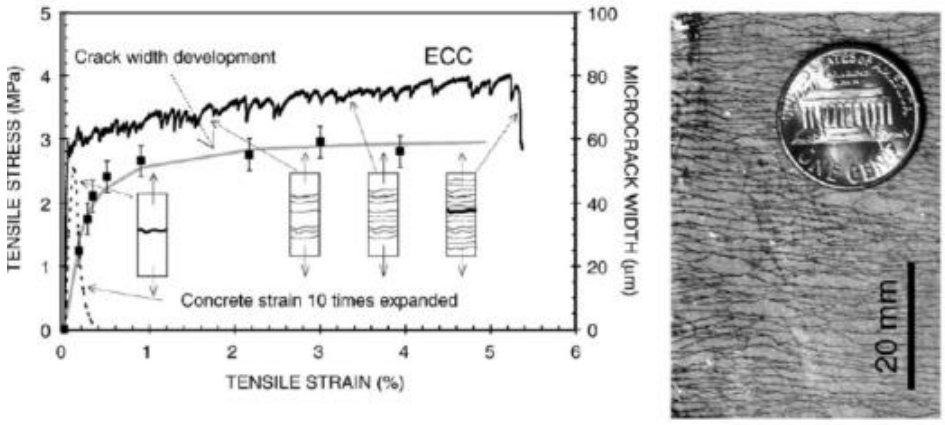

Figure 2-5 Properties of ECC (Şahmaran et al., 2009)

2.7. Effects of Short fibers in the Matrix

The addition of short fibers to a matrix of concrete can have several effects on its mechanical performance. For example, short fibers act as a dispersed reinforcement inside matrix material, improving its tensile strength. Short fibers resist crack propagation and provide extra resistance against tensile forces. Thus, this improved tensile strength helps to avoid the formation and widening of cracks in the material. First crack stress and the ultimate tensile strength of TRC specimens increased substantially by the different of concrete matrix (Esmaeili et al., 2017).

In addition to that, the presence of short fibers improves the crack resistance and control of the matrix material. Fibers can act as crack arrester, avoiding crack propagation and limiting crack widths. This can be favourably taken into account where crack control is critical, such as structural elements subjected to tensile loads or flexural.

Likewise, short fibers can improve the toughness and energy absorption capacity of the matrix material. The fibers can unleash energy by bridging cracks and absorbing applied loads. Hence, it can result in more ductile behavior and enhanced ability to withstand impacts and dynamic loads.

In addition to that, the addition of short fibers can help mitigate the impact of shrinkage. These fibers can act as internal reinforcements, decreasing the formation of shrinkage cracks and minimizing their widths. This is especially important in places where minimizing crack widths and controlling shrinkage-induced cracking are essential, such as reinforced concrete buildings.

It is necessary to note that the effectiveness of short fibers in the concrete matrix related to factors such as fiber type, fiber volume fraction, along with suitable mix design and manufacturing techniques, are necessary to obtain the expected mechanical properties and performance of fiber-reinforced composite. Table 2-1 below presents the properties of some short fibers that are typically used in fiber reinforced concrete production.

Table 2-1 Mechanical Properties of Fibers (*Aydınç Güzelce* 2019;Keskin 2012)

Fiber Type	Steel	PP	Nylon	Carbon	Glass	PVA
Tensile Strength (kN/mm^2)	0.5-2	0.5-0.75	0.9	2.6	2-4	1-1.6
Modulus of Elasticity (GPa)	200	5-7	4	230	70-80	40-45
Elongation at break (%)	0.5-3.5	8	13-15	1	2-3.5	6-6.5
Diameter (μm)	5-500	20-200	-	9	9-15	35-45
Density (10^3 kg/m3)	7.84	0.9	1.1	1.9	2.6	1.3

2.7.1. Steel Fibers

Steel fibers are typically made from low carbon steel and are added to concrete mixture to improve its mechanical properties. Steel fibers have various shapes, including hooked, crimped, or straight to increase their bonding with the concrete matrix (Sengun et al., 2023). Furthermore, steel fibers act as a dispersed reinforcement in the concrete matrix. They are uniformly distributed to concrete mixture to enhance the mechanical properties such tensile strength, toughness, and crack resistance (Batson, 1976).

Steel fibers provide a 3-D reinforcement network that supports controlling crack propagation and improves the overall performance of the concrete. Additionally, these fibers also enhance the post-cracking behavior of concrete by bridging cracks and distributing stress, leading to improved load-carrying capacity. Steel fibers are traditionally used in different applications, including industrial floors, precast elements, shotcrete, tunnel lining and overlays.

Steel fibers are particularly crucial in areas where high impact resistance, crack control and high flexural strength are necessary. Besides, proper mixing and dispersion of steel fibers in the concrete mixture are important for achieving uniform distribution and effective reinforcement. Mixing techniques, such as high energy mixing or fiber pre-blending, may be needed to make sure proper dispersion of the fibers throughout the concrete mix.

2.7.2. PP Fibers

Polypropylene fibers, often referred to as PP fibers, constitute a type of synthetic fibers commonly used reinforcement in concrete and other cementitious materials. PP fibers are made of 100% virgin polypropylene resin. They can be found in various forms, include monofilament fibers (single strand) and fibrillated fibers (multiple small strands that form a network). These fibers are normally thin and range in length from a few millimeters to several centimeters.

Usually, PP fibers act as a secondary reinforcement in concrete and cementitious materials. PP fibers are added to improve the materials post-cracking performance and durability. The fibers disperse throughout the matrix to provide distributed reinforcement and enhance the properties such as crack control, durability, and impact resistance(Das et al., 2018). In addition, PP fibers can control crack formation and restrict crack widths in concrete. They distribute stress and enlarge the materials resistance to plastic shrinkage, settlement, and drying shrinkage cracking. Moreover, it improves the durability of the cementitious materials. And it can increase resistance to freeze-thaw cycles, lessen permeability, and diminish the effect of harmful substances into concrete. They help to reduce the ingress of water, chloride ions, and improve the long-term performance and service life.

PP fibers are in some ways easier to handle and mix into concrete. They can distribute easily and uniformly throughout the mix with proper mixing techniques. PP fibers are generally applied to various concrete structures and elements, such as shotcrete, precast elements, and architectural concrete.

2.7.3. PVA Fibers

Polyvinyl Alcohol fibers also known as PVA, are a type of synthetic fiber used as reinforcement in different applications, including concrete and cementitious materials. PVA fibers are derived from polyvinyl alcohol, which is a synthetic polymer that readily dissolves in water. PVA fibers are traditionally manufactured by a wetting

process. They can be found in different forms, including monofilament fibers (single-strand) and multifilament fibers (multiple strands bundles together).

When these fibers are added to improve the mechanical behavior of concrete, especially the tensile strength and crack control capabilities, their surface is coated so that it does not dissolve in water. They are typically preferred in ECC production, where they are efficient in crack control and mitigation. It can improve the resistance to plastic shrinkage cracking, settlement cracking and drying shrinkage cracking(Zhang et al., 2022). Moreover, PVA fibers have tensile strength that can help to the improved mechanical property of the composite material. PVA fibers assist to distribute the applied loads and provide additional reinforcement against tensile forces. Finally, it can result in enhanced flexural strength and resistance to cracking.

When they are exposed to water or moisture, PVA fibers slowly dissolve and disintegrate. Hence, this property can permit fibers to break down during the curing process, leaving behind voids that can increase the materials freeze-thaw resistance and permeability. PVA fibers are generally applied to precast elements, shotcrete and for the structures where crack control and durability are crucial to control. And they can be also used in non-structural applications such as textiles, packaging materials and paper.

2.7.4. Nylon

Nylon is a thermoplastic material made from the condensation polymerization of monomers. Nylon has excellent mechanical strength which makes it a strong and durable material. Nylon offers a good resistance to wear, impact and abrasion and makes it appropriate for applications where durability and strength are needed(Ahmad et al., 2021).

Moreover, Nylon has a relatively high melting point compared to other polymers, giving it good thermal stability and resistance to high temperatures. This type of fiber can keep its mechanical properties even at elevated temperatures. Thus, it can make them suitable for applications that involve exposure to heat.

Furthermore, Nylon can show good resistance to many harmful chemicals, including solvents, oils greases and alkalis. This chemical resistance permits nylon to be utilized in applications where exposure to different substances is anticipated. Due to low coefficient of friction, it has an excellent sliding property. Besides, it is also self-lubricating, thereby decreasing the requirements for supplemental lubrication in specific applications. Nylon is used in various industrial sectors. Some of the common applications are textiles and fabrics, engineering plastics, electrical and electronic applications, and packaging.

CHAPTER 3

EXPERIMENTAL PROGRAM

3.1. General

The main objective of this thesis study is to investigate the effect of matrix types containing different amounts of short steel and PVA fibers, when used with a carbon textile in the weft direction, on the mechanical properties of Carbon Textile Reinforced Cementitious Composites (C-TRCC). With this in mind, a leno weaved carbon textile structure is used with two basic types of matrices utilizing different binder types and amounts. The toughness of the two basic matrices were also increased by the utilization of either short steel or PVA fibers. In this chapter, the materials and methods used in the experimental program will be provided.

3.2. Materials

In all of the cementitious mixtures, Portland cement, fly ash, siliceous sands with different particle size distributions, short steel or PVA fibers, and a superplasticizing chemical admixture were used together with a carbon textile as the main reinforcement. The properties of these materials are explained below.

3.2.1 Cement

CEM I 42.5 R type of Portland cement produced according to the EN 197-1 standard by Baştaş Çimento A.Ş. is used in all of the cementitious mixtures. The chemical analysis of the cement is determined by TURKCIMENTO and presented in Table 3-1. The physical properties together with the compressive strength of the cement is determined by following the relevant standards in the Materials of Construction Laboratory of METU Civil Engineering Department, and is presented in

Table 3-2.

Table 3-1 Chemical Analysis Results of the Portland cement

Chemical Composition	(%)
SiO_2	18.32
Al_2O_3	4.48
Fe_2O_3	2.84
CaO	61.3
MgO	1.59
SO_3	2.78
Na_2O	0.28
K_2O	0.81
Cl^-	0.04
Loss on Ignition (LoI)	6.82
Insoluble Residue (IR)	0.76

Table 3-2 Physical and Mechanical Properties of the Portland Cement

Specific Gravity		3.10	ASTM C150
Blaine Fineness (cm^2 /g)		3411	ASTM C204
Initial Setting (min)		165	ASTM C191
Final Setting (min)		215	ASTM C191
Compressive Strength (MPa)			ASTM C109
	2 Days	20.7	
	7 Days	31.4	
	28 Days	43.7	

3.2.2 Siliceous Sand

Sieve analysis for the siliceous sands having two different particle sizes is carried out according to ASTM C136-06. In addition, specific gravity and water absorption tests are carried out according to ASTM C127-15. All the relevant tests are conducted in the Materials of Construction Laboratory of METU Civil Engineering

Department. The physical properties for both types of siliceous sand are given in Table 3-3 and the sieve analysis is shown in Figure 3-1.

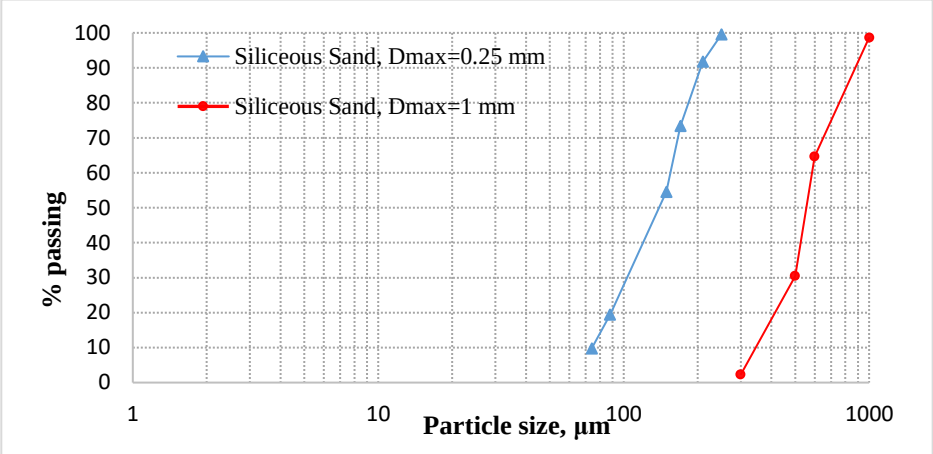

Figure 3-1 Particle size distribution of the two siliceous sands

Table 3-3 Physical Properties of Siliceous Sands

Properties	D_{max}=1 mm	D_{max}=0.25 mm
Specific Gravity (Saturated Surface Dry)	2.56	2.65
Specific Gravity (Oven Dry)	2.57	2.67
Specific Gravity (Apparent)	2.59	2.69
Water Absorption (%)	0.54	0.60

3.2.3 Chemical Admixture

A commercially available high-range water-reducing admixture, MasterGlenium 51, is used as a chemical admixture in all mixtures. The properties as provided by Master Builders Solutions company is presented in Table 3-4.

Table 3-4 Properties of the superplasticizer

Structure of the Material	Modified Polycarboxylate Ether Based
Appearance	Brown liquid
Specific gravity @ 20°C	1.082 - 1.142 kg/lt
PH-value	6-7
Alkali content (%)	≤ 3.00 (by mass)
Chloride content (%)	≤ 0.100 (by mass)

3.2.4 Fly ash

In order to improve the cementitious matrix, fly ash of type F is used in the ECC base matrix. It was a by-product of the Sugözü Thermal Power Plant which has a specific gravity of 2.10. The properties that are provided in

Table 3-5 are determined by TURKCIMENTO.

Table 3-5 Chemical properties of the fly ash

Chemical Composition	(%)
SiO_2	58.5
Al_2O_3	22.0
Fe_2O_3	6.41
CaO	3.13
MgO	2.15
SO_3	0.28
Na_2O	1.0
K_2O	1.39
TiO2	0.92
Loss on Ignition (LoI)	3.34

3.2.5 Water

Tap water available in the METU-CE Materials of Construction Laboratory is used in all the mixtures.

3.2.6 Textile

In this study, carbon textile that was obtained from the Solidian Company, Germany was used which was labelled as “FLEX GRID-CAR-260-CCS1-14x14”. The properties of the textile as obtained from the manufacturer are shown in Table 3-6.

Table 3-6 Properties of the Carbon Textile Provided by the Manufacturer

Property	*Direction*	*Unit*	*Tolerance*	*Value*
Basis Weight	-	g/m^2	± 5%	260
Cross-Section of the Strands	Warp	mm^2	-	0.9
	Weft	mm^2	-	0.9
Cross-Section of the Reinforcements	Warp	mm^2/m	-	54
	Weft	mm^2/m	-	54
Mesh size (Middle)	Warp	mm	± 0.5%	16.7
	Weft	mm	± 0.5%	16.7
Tensile Strength	Warp	kN/m	-	126
	Weft	kN/m	-	120
Impregnation Material	Styrene-butadiene (>18)			

It was manufactured in two orthogonal directions (named as warp and weft) at a nominal spacing of ($16.7x16.7mm^2$), as can be seen in Figure 3-2. The yarns along the length of the textile are called the warp yarns and those along the width are called the weft yarns. According to the manufacturer, the warp yarns had an average count of 800×2 tex, while the weft yarns had a count of 1600 tex, which were both impregnated with styrene-butadiene. Styrene-butadiene is a chemically crosslinking material which result in an increased mechanical performance and bond behavior (Heins et al., 2023b).

Moreover, as depicted in Figure 3-3, during the manufacturing of the carbon textiles the longitudinal warps yarns are split into two and the weft yarn crosses in between those split yarns at each knot. In order to strengthen the knots, a spiral glass yarn is also leno-weaved through the warp yarn which was visible in Figure 3-3. This is reported to be used to prevent the deflection of the knots of the textiles and stabilize the efficiency of textiles (Heins et al., 2023a).

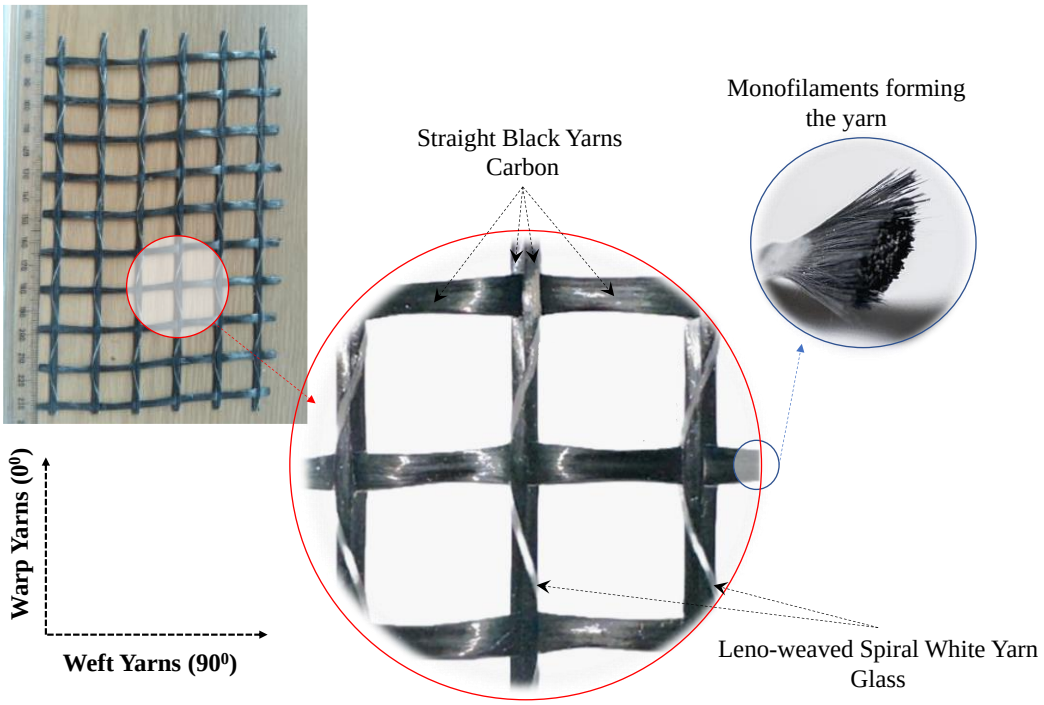

Figure 3-2 The carbon textile utilized in this study

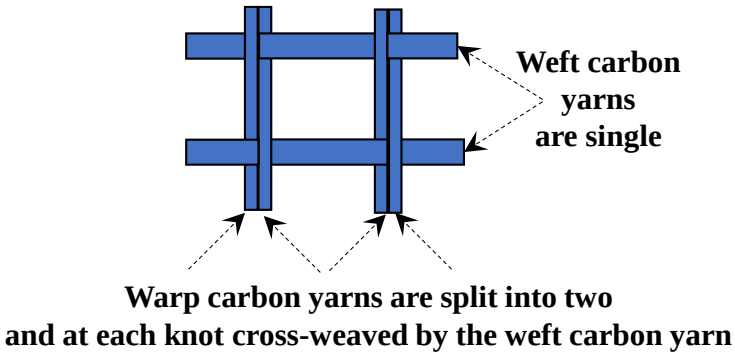

Figure 3-3 Weaving pattern of the carbon textiles

In addition to the information provided by the manufacturer, a uniaxial tensile test of the yarn in the weft direction is conducted at the Materials of Construction Laboratory of METU's Department of Civil Engineering. In this test, a 300 mm long yarn was tested under uniaxial tension under displacement-controlled loading scheme at

a rate of 0.5mm/min. Moreover, while gripping both ends of the yarn, it was held by two 7*7 cm^2 aluminum plates to prevent slippage and failure due to stress concentration at the ends of the tensile grip fixtures. Sufficient lateral pressure was applied to the grips to prevent damage to the carbon yarn. The stress that would occur on the yarn was obtained by diving the applied load by the cross-sectional area of the yarn, and the strain is obtained by dividing the free length to the displacement. The results are shown in Figure 3-4 and Table 3-7.

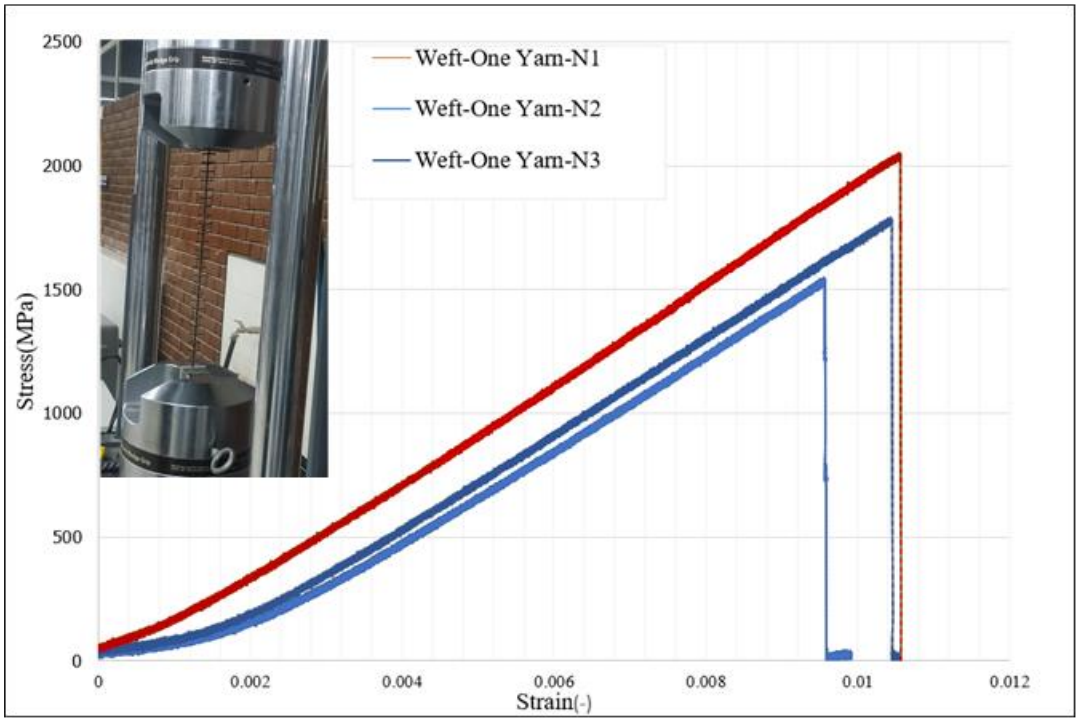

Figure 3-4 Uniaxial Tensile Test on Carbon Textile

From that figure, the strength and the effective modulus of elasticity of textile, E_t, is computed (Table 3-7) as the secant modulus between 20 and 60% of maximum stress according to ACI 434 as follows:

$$E_t = \frac{0.4\sigma_{f,ult}}{\varepsilon_{f@0.6\sigma_{f,ult}} - \varepsilon_{f@0.2\sigma_{f,ult}}}$$

where;

$\sigma_{f,ult}$ is the tensile strength of the textile

$\varepsilon_{f@0.6\sigma_{f,ult}}$ and $\varepsilon_{f@0.2\sigma_{f,ult}}$ are the strains at 60% and 20% of textile tensile strength.

Table 3-7 Tensile testing of the weft yarn of the carbon textile

Specimen #	Modulus of Elasticity (GPa)	Tensile Strength (MPa)	Strain at Maximum Stress
1	206	2010	0.011
2	193	2012	0.009
3	196	1780	0.011
Mean	**198.3**	**1934.0**	**0.010**
CoV (%)	**3**	**6**	**11**

As realized in that Figure 3-4 there is a nonlinear initial part in the stress-strain diagram of the yarn. This was explained by Valeri et al (2020) as the straightening of the yarns during tensile testing as shown in Figure 3-5.

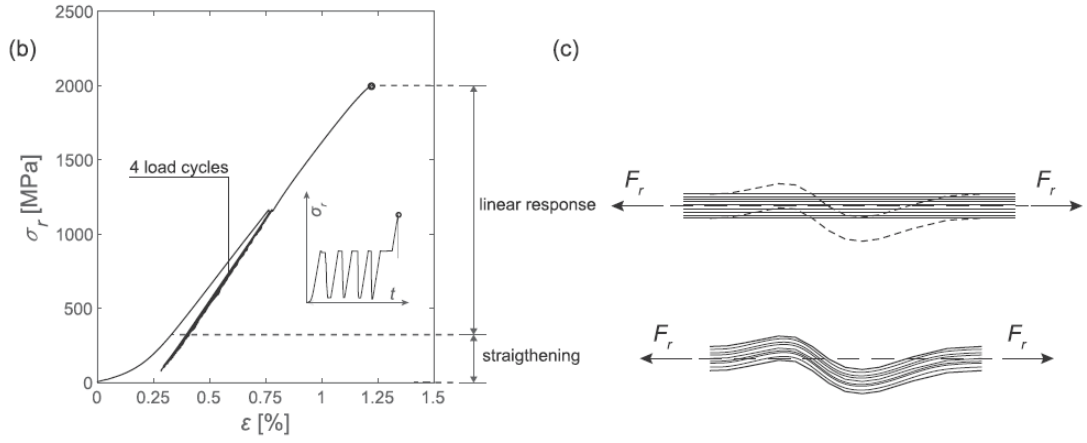

Figure 3-5 Straightening of the yarns during uniaxial tensile testing (Valeri et al., 2020)

3.2.7 Short Steel Fibers

Due to the restricted opening size of the meshes of carbon textile, copper-coated steel fibers with a length of 6mm are utilized. The properties of steel fibers declared by the manufacturer can be found in Figure 3-6.

Steel Fibers (Dramic OL 6/16)	
Tensile Strength(MPa)	2000
Length (mm)	6
Diameter (mm)	0.375
Length/Diameter	16
Density(kg/m3)	7170

Figure 3-6:The properties of steel fibers

3.2.8 PVA Fibers

PVA fibers with a special coating are used for ECC matrix. These fibers are coated with 1.2% hydrophobic oiling agent by mass. The properties of PVA fibers can be found in Figure 3-7 as provided by the manufacturer.

Tensile Strength(MPa)	1092
Length(mm)	8
Diameter(mm)	0.039
length/Diameter	205
Density(kg/m^3)	1300

Figure 3-7 Properties of PVA fibers

3.3. Experimental Procedures

3.3.1. Mix Proportions

Carbon textile had a relatively small mesh opening and as the fibers were to be used, a highly flowable and a cohesive cementitious mixture was prepared by slightly modifying the M7 mixture proposed by (Textile Fibre composite in civil Engineering, Page 28.) with a cement content of 890 kg/m3. Moreover, to investigate the effect of a different matrix a mixture was decided on the basis of ECC mixture proportions widely presented in the literature (Keskin, 2012), also known as M45. The mixture proportions of M7 and ECC are given in Table 3-8 and Table 3-9 respectively.

Both mixtures had a relatively low w/c and a Polycarboxylate ether type high-range water reducer was utilized. When the fiber dosage was increased from 1% to 2%, an increase in the chemical admixture was necessary to achieve the required consistency and to prepare a cohesive and self-compacting concrete. The workability of M7 matrix was measured by using V-funnel between 7-9 seconds according to ASTM C1610.

Table 3-8 Mix proportions of the M-7 matrix

Materials	**Mix 1 (V_f=0%)**	**Mix 2 (V_f =1%)**	**Mix 3 (V_f =2%)**
Cement, (kg/m^3)	890	890	890
Siliceous Sand (0.25mm), (kg/m^3)	534	523	517
Siliceous Sand (1 mm), (kg/m^3)	534	523	517
Steel Fibers, (kg/m^3)	0	79	157
Water, (kg/m^3)	267	267	267
SP, (kg/m^3)	11.6	11.6	15.0
W/C ratio	0.30	0.30	0.30

Table 3-9 Mix proportions of ECC matrix

Materials	**Mix 1 (V_f =0%)**	**Mix 2 (V_f =1%)**	**Mix 3 (V_f =2%)**
Cement, (kg/m^3)	557	557	557
Fly ash, (kg/m^3)	668	651	641
Siliceous Sand (0.25mm), (kg/m^3)	445	434	427
PVA Fibers, (kg/m^3)	0	13	26
Water, (kg/m^3)	361	361	361
SP, (kg/m^3)	6.7	11.0	26.0
W/B ratio	0.29	0.29	0.29

The mixing procedure was also kept similar. First, siliceous sands and cement were mixed for two minutes. Water was then slowly added to the matrix for 1 minute to achieve a workable matrix. The superplasticizer was dispersed by part of the mixing water to obtain a homogeneous mixture. Finally, fibers were added. Then the matrix was mixed for an additional 2 minutes to mix the fibers uniformly in the matrix. The materials that are explained above, were mixed together in a planetary mixer of 25 L capacity (Figure 3-8) in order to achieve a homogeneous mixture.

Figure 3-8 Concrete batching mixer

3.3.2. Specimen Preparation

Prior to casting concrete, carbon textile was cut with scissors then they were clamped to both sides of a specially manufactured formwork shown in Figure 3-9 and Figure 3-10. The formwork was equipped with an external vibrator and designed such that TRCC mixtures can be molded to a specific clear cover.

Due to the low workability of ECC and M7 matrices especially for 2% fibers, laminating technique was used for the preparation of TRC specimens as shown in Figure 3-12. This technique is applied to TRC elements in which the fine-grained concrete and the textile are alternately inserted into the formwork layer by layer until the component thickness is obtained (Textile Fibre & Civil Engineering, PP.48.). In one batch a total of 10 specimens were prepared; 5 specimens with 1 layer of textile and another 5 specimens with 2 layers of textile as can shown in Figure 3-11.

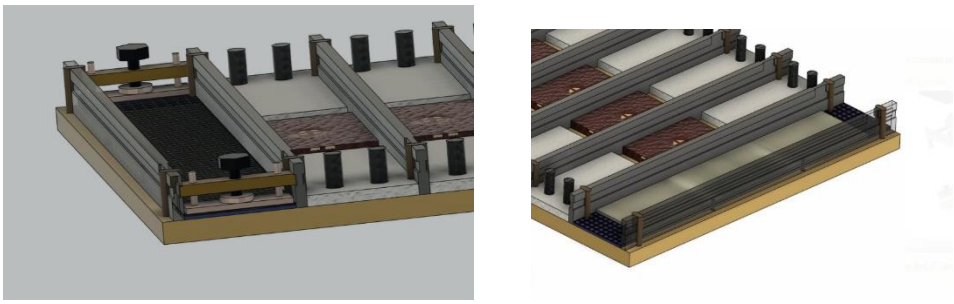

Figure 3-9 3-D Drawing of the Formwork

Figure 3-10 Clamping of Textile in the Formworks

Figure 3-11 Formwork used for the preparation of fresh TRC specimens.

Figure 3-12 Laminating Technique for casting of ECC matrix

The specimens are demolded the next day, and then cured for 28 days in a pool having a temperature of 23 ± 2 °C. A typical picture showing the curing process of the specimens can be found in Figure 3-13.

Figure 3-13 Pool for Curing of TRC Specimens

After 28 days in the pool, the specimens were ready for testing. For the tensile test, 200x100x4 mm^3 steel plates were bonded to TRC specimen ends by using a special Weber EP adhesive. This is a solvent free epoxy-based repair, anchoring and fitting mortar. The advantage of using this epoxy is that it is easy to mix and apply, has high mechanical properties and is chemical resistant. The application of the epoxy and the steel plates are shown in Figure 3-14. The specimens were then sprayed with white colour to be ready for Digital Image Correlation (DIC) to measure the deformation of the specimen using the area of interest on the specimens. The application of the white colour spray is shown in Figure 3-15.

Figure 3-14 Bonding of Steel Plates with Epoxy to the Ends of Specimens

Figure 3-15 View of white-colored spray for DIC analysis

3.3.3. Uniaxial Tensile Test Setup

Uniaxial testing was performed using an MTS Landmark Series 250 kN capacity load cell. Loading was applied using a displacement-controlled loading scheme at a rate of 0.5 mm/min. A clevis grip tensile test setup was used as shown in Figure 3-16. In a clevis grip, two metal tabs are bonded to each end of the C-TRCC specimen and loading is transferred through the metal tabs to the specimen being tested. The setup is designed to minimize eccentricity by using spherical ball bearings (hinge joints) at both ends. All C-TRCC specimens were tested in the weft (90°) direction of the carbon textile. The typical view and the components and dimensions of the C-TRCC specimen are shown in Figure 3-17.

Figure 3-16 Uniaxial Tensile Test Setup

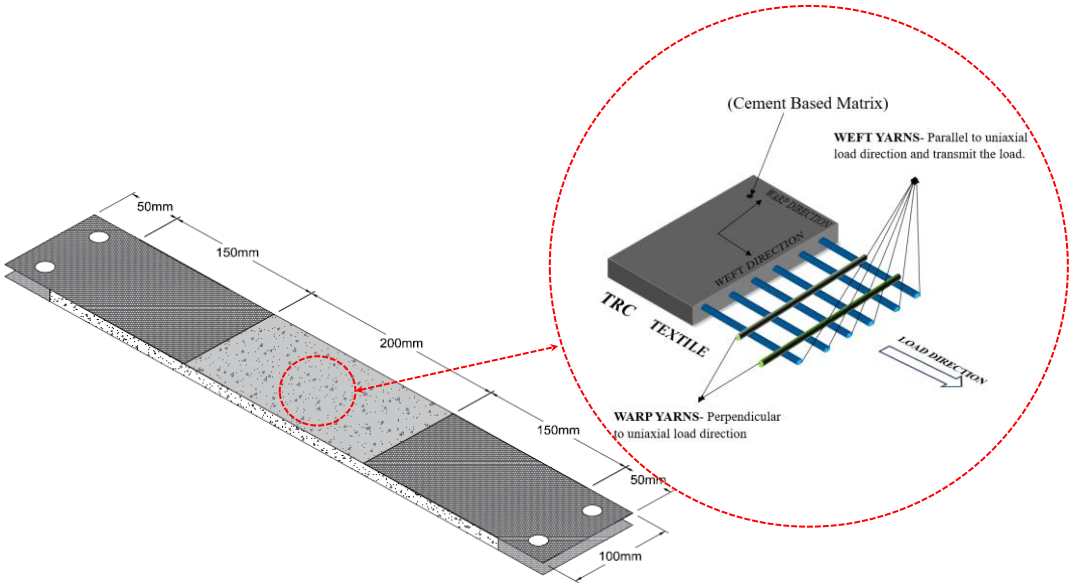

Figure 3-17 The components and the dimensions of a typical C-TRCC

After testing the C-TRCC specimens in uniaxial tension, the steel plates that were bonded with the epoxy resin was baked in a furnace at 350ºC. Later, using simple tools the epoxy was scraped from the steel plates to be reused in the next casting. The burning of the epoxy and steel plates is shown Figure 3-18.

Figure 3-18 Removal of epoxy from steel plates

3.3.4. Analysis of the Uniaxial Tensile Test Data

After performing the uniaxial tests on the C-TRCC specimens, the data, which was obtained was used for analyzing the load-deformation plot of each specimen. The software MATLAB was used for this analysis.

The analysis is adopted from the AC434 guidelines as described by De Santis et al. (2018). This guideline suggests that the mechanical properties of TRCC are obtained from tensile tests performed on a clevis type grip. In this test method, an axial load is applied from a universal test frame through clevis grips. The TRCC specimen is connected to the clevises by two sets of metal tabs bonded to its ends.

By using the script in MATLAB code, the following parameters are obtained from the clevis grip tensile test on TRCC specimens (Figure 3-19):

- The textile stress (σ_f) and the normalized deformation ($\frac{\Delta L}{L_0}$) plot for the specimen is plotted.
- Ultimate tensile strength observed on the textile, σ_{f_u}, is calculated as:

$$\sigma_{f_u} = \frac{F_{max}}{A_f}$$

  here, F_{max} is the ultimate force experienced by the TRCC specimen, and A_f is the cross-sectional area of the textile.
- Tensile modulus of elasticity of the cracked TRCC specimen, E_f, is calculated as:

$$E_f = \frac{0.3 * \sigma_{f_u}}{\varepsilon_{f_{@0.9\sigma_{f_u}}} - \varepsilon_{f_{@0.6\sigma_{f_u}}}}$$

  here, $\varepsilon_{f_{@0.6\sigma_{f_u}}}$ and $\varepsilon_{f_{@0.9\sigma_{f_u}}}$ are the strains that correspond to $0.6\sigma_{f_u}$ and $0.9\sigma_{f_u}$ in the load-normalized deformation curve.

- Ultimate tensile deformation of TRCC specimen, ε_u, is calculated as:

$$\varepsilon_u = \varepsilon_{f_{@0.6\sigma_{f_u}}} + \frac{0.4\sigma_{fu}}{E_f}$$

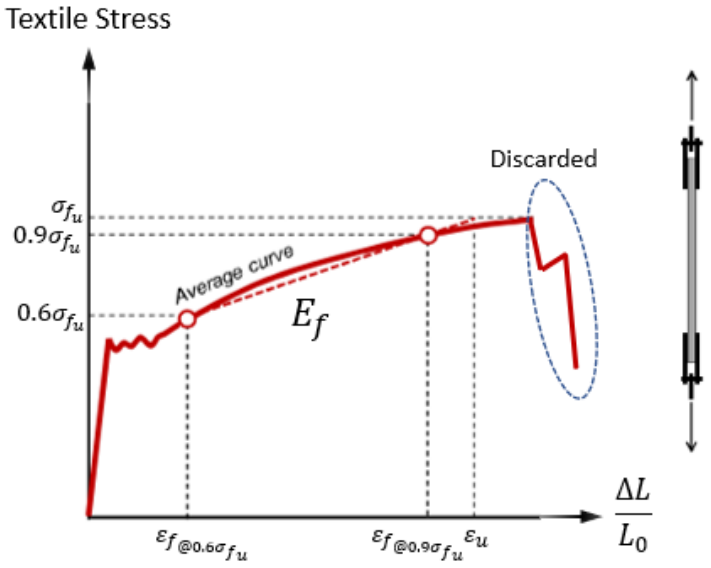

Figure 3-19 Response stage of TRCC under textile loading for clevis-grip specimens(De Santis et al., 2018)

For the displacement measurements, a video extensometer was used that calculates the average axial strain (AVE) from 100 mm of gauge length, as shown in Figure 3-20. However, due to the inherent sensitivity of the AVE after the first crack and the limited coverage of the AVE, the MTS displacement data was considered in the calculation of the deformations and the deformation was assumed to occur within the 200 mm region of interest. To improve the validity of this assumption, the two steel plates used in the test setup were welded together and the stiffness of the test setup was obtained under uniaxial loading, as shown in Figure 3-21. Later, the displacement along the region of interest was obtained by subtracting the steel plate displacement at each load increment from the MTS displacement data.

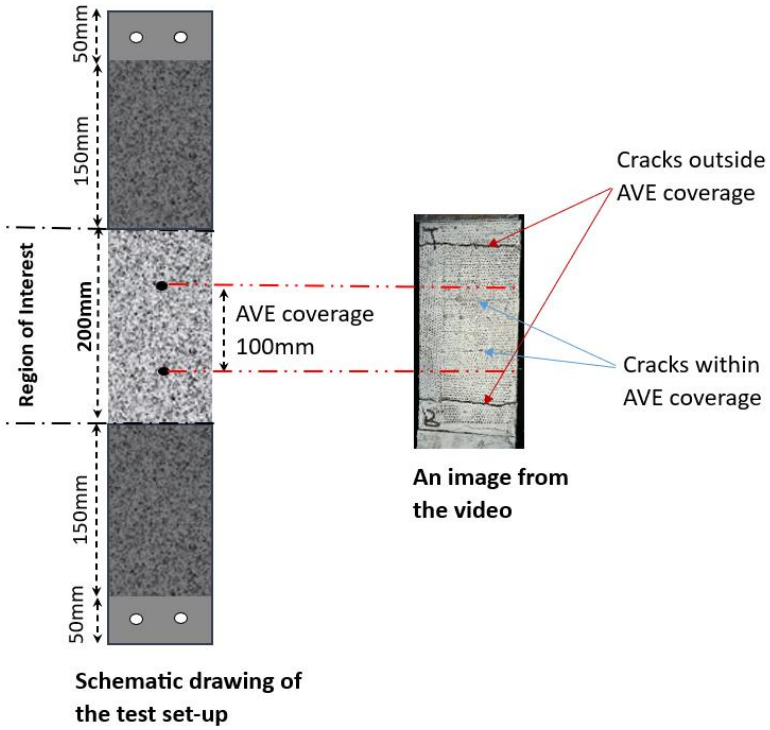

Figure 3-20 AVE measurement for TRC specimen

Figure 3-21 Uniaxial testing of the steel plates alone

Finally, taking into account ACI 434 recommendations, the data that was assumed to be due to slippage of the core filaments from the sleeve filaments were removed from each load-normalized deformation plot after the ultimate strength of the C-TRCC specimens, as shown Figure 3-22. Note that, when necessary, DIC analysis was also used to explain the crack formations in the C-TRCC specimens.

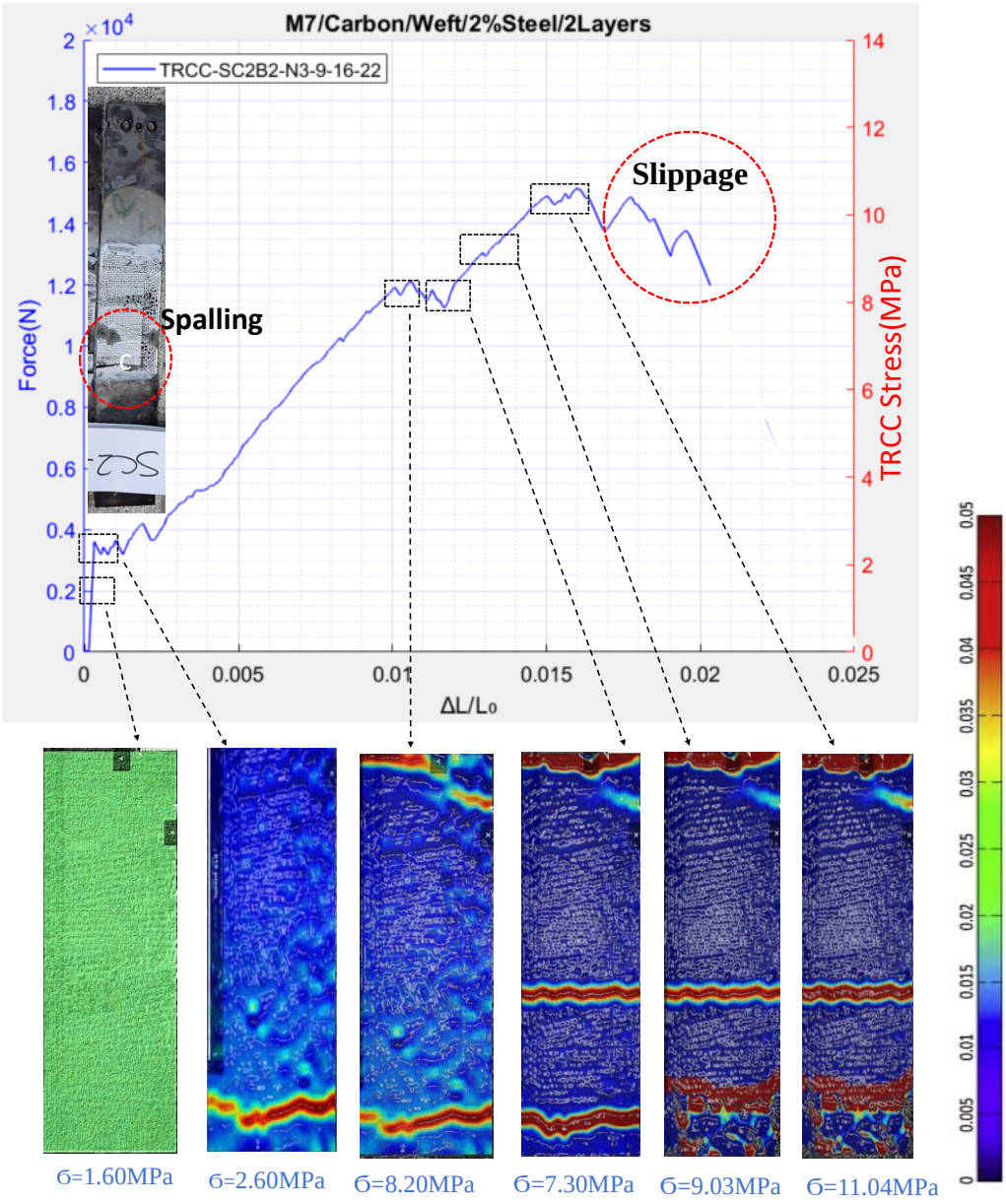

Figure 3-22 Sample graph for slippage

3.3.5. Compressive Strength Tests

Compressive strength tests are performed using the UTEST UTCM3742.FPR Automatic Cement Flexure/Compression Testing Machine and in accordance with ASTM C-109. The compressive strength test results are compared with the reference sample to ensure the increase in strength due to the amount of fibers. In this experiment, three 50*50*50 mm cube specimens were prepared for each casting. After 28 days in the pool, the specimens were tested. The loading rate was 0.05kN/Sec for all the cube specimens. The maximum stress was obtained by dividing force by the cross-sectional area of the specimen.

CHAPTER 4

TEST RESULTS AND DISCUSSIONS

4.1. General

In this chapter the analysis of C-TRCC specimens under uniaxial tension will be presented for both matrices separately after first reviewing the behavior of the carbon textiles in TRCC. All the tensile load-normalized deformation data for C-TRCC specimens are presented in Appendix B for the M7 matrix, and in Appendix C for the ECC matrix.

4.2. The Behavior of Carbon Textiles in TRCC

Textile reinforcement serves as the primary source of tensile strength and ductility in TRCC. During the production of textiles, several surface treatment procedures could be applied and the yarns are typically impregnated or coated with cement- or polymer-based matrices to create a composite material that increase the strength of the individual monofilament fibers as well as their durability. In addition, it has the purpose of stabilizing the inner structure of the yarn by fixing and shaping of the textile. Figure 4-1presents the surface treatment procedures in textile yarns and the stress distribution in the yarn under uniaxial tension. When the coating is applied to impregnate the whole yarn, the activation of inner filaments increase and the stresses are uniformly distributed to all monofilaments. Without full impregnation, the behaviour within the yarn cross-section will not be uniform, and the monofilaments will exhibit different tensile stresses as depicted in that figure.

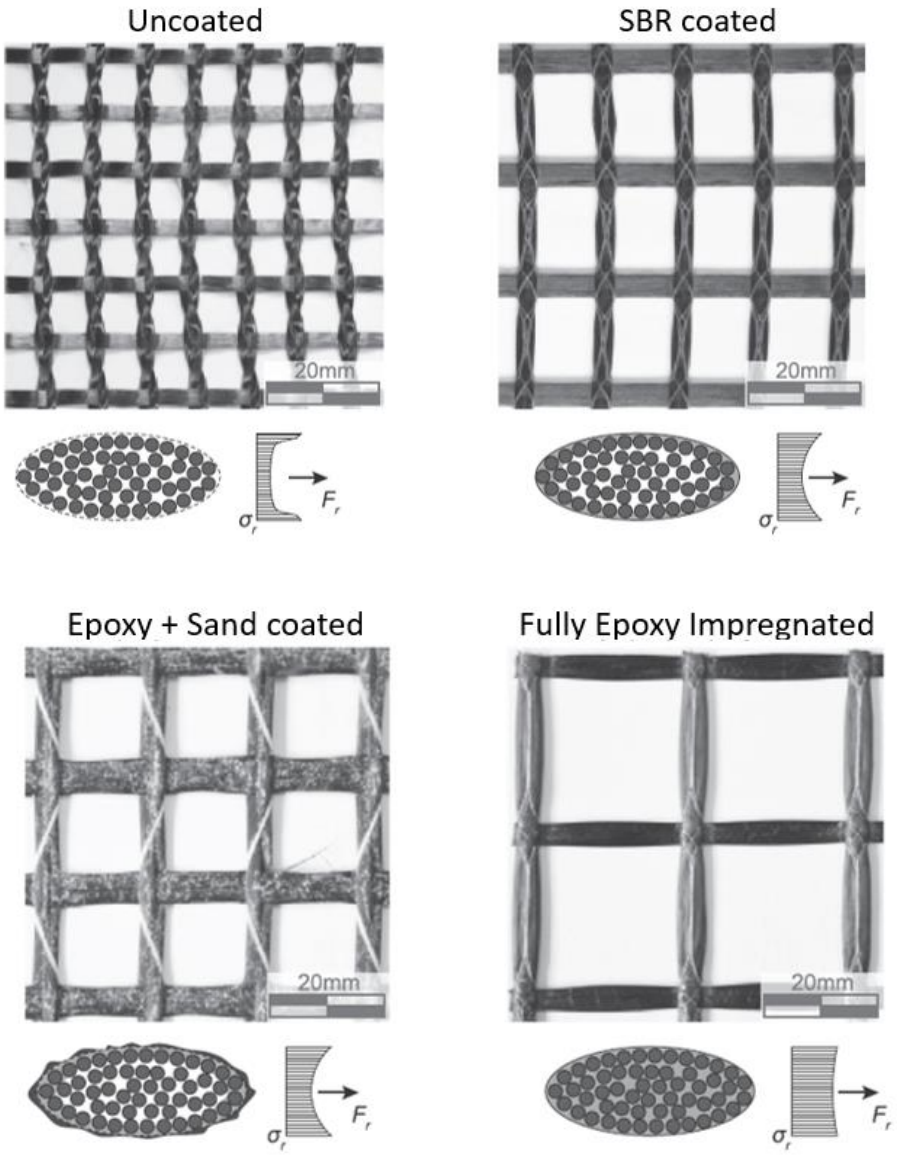

Figure 4-1 Typical surface treatment possibilities in textiles (Valeri et al., 2020)

As the carbon textile that was tested had many monofilaments within one yarn and an epoxy resin (Styrene-butadiene) coating was applied on the surface of the yarn, the two distinct layers can be identified within the structure:

- ***Sleeve filaments***: These filaments are in direct contact with the cementitious matrix. The sleeve filaments layer experiences higher levels of stress and friction, leading to the initiation of breaks before the other layers.

- ***Core filaments***: These filaments are in contact with other filaments within the textile. As sleeve filaments begin to fail, the core filaments had already slipped, facilitated by reduced frictional resistance.

Therefore, under uniaxial tensile tests which are performed in a clevis type of loading, the failure in the textile starts with the failure of the outer filaments. After the external filaments fail, a telescopic type of pullout is generated, whereby the internal (core) filaments slip against the external (sleeve) filaments. This systematic layer-by-layer displacement process, as illustrated in Figure 4-2 is known as "telescoping failure" (Peled et al., 2017; Texile Fibre &civil Engineering, P.77).

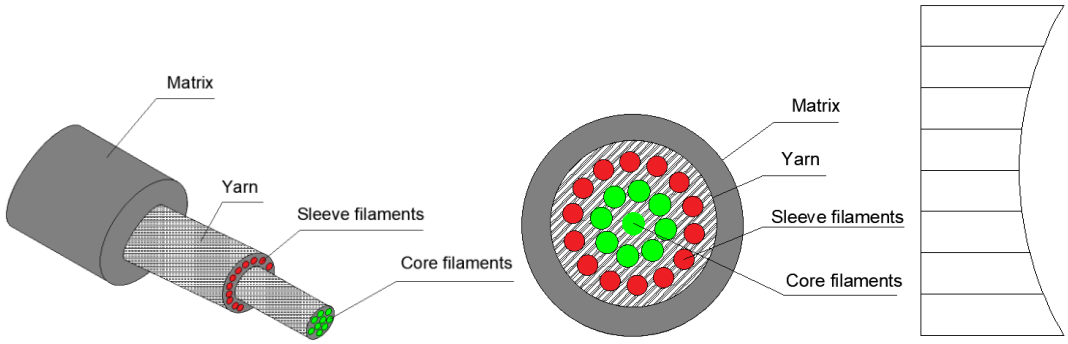

Figure 4-2 Typical depiction of the telescoping nature textile and stress distribution

Therefore, when carbon textile is embedded into to a cementitious matrix, a separation of outer filaments from the yarn bundle occurs causing a slippage-like deformation within the yarn. Because of this slippage phenomenon, in the uniaxial testing of the C-TRCC specimens the normalized deformation values were higher than the tensile strain capacity of the textile which was around 1.2%. This was the case in other related literature (Giorgia et al., 2013; Heravi et al., 2020; Zhu et al., 2019).

4.3. Characterization of C-TRCC with the M7 Matrix

The uniaxial compressive and tensile strength testing of the M7 matrix was first performed and the results are presented in Table 4-1. Even though the change in compressive strength with steel fiber amount is not that clear, the change in the tensile

strength was more visible. It should also be mentioned that the amount of variability is rather high especially when the steel fiber volume is increased.

Table 4-1 The characteristics of the M7 matrix in the absence of textiles

% steel fibers by volume	**Compressive Strength (MPa)**		**Tensile Strength (MPa)**	
	Mean	**CoV (%)**	**Mean**	**CoV (%)**
0	75	6	4.4	6
1	70	8	4.8	9
2	79	6	5.2	15

Moreover, when the load-normalized deformation plots (characteristics are summarized in Table 4-2) provided in Appendix B, is analyzed it can be seen that all specimens exhibited a single crack leading to brittle failure. However, with increased steel fiber percentage a slight strain softening behavior was observed especially when the fiber volume was increased to 2%.

Table 4-2 M7 Control Specimens, [] shows the CoV in %

Mix ID	Steel Fiber Dosage	Thickness (t)	First Crack Strength (σ_{cr})	Ultimate Strength (σ_u)	$\Delta L/L_0$ at σ_u	Max $\Delta L/L_0$	F_{max}
	(%)	(mm)	(MPa)	(MPa)	-	-	(kN)
M7	0	16.0 [0.04]	4.4 [6]	4.4 [6]	0.00037 [6]	0.00037 [6]	6.9 [3]
	1	16.1 [0.09]	4.8 [9]	4.8 [9]	0.00038 [8]	0.00041 [22]	7.8 [18]
	2	17.9 [0.05]	5.2 [15]	5.2 [15]	0.00043 [16]	0.00157 [83]	9.3 [13]

After characterizing the M7 matrix, the mechanical properties of the C-TRCC specimens that had 1 and 2 layers of textiles were analyzed. Figure 4-3 presents the results for 1 and 2 layers of textiles when the M7 matrix contain different amount of steel fibers.

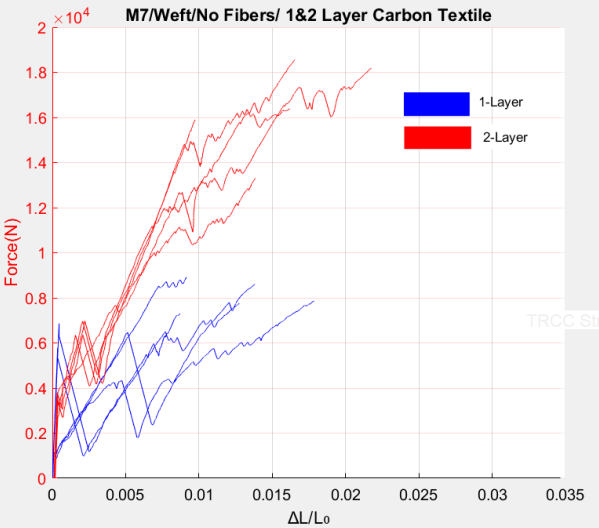

(a) No steel fibers

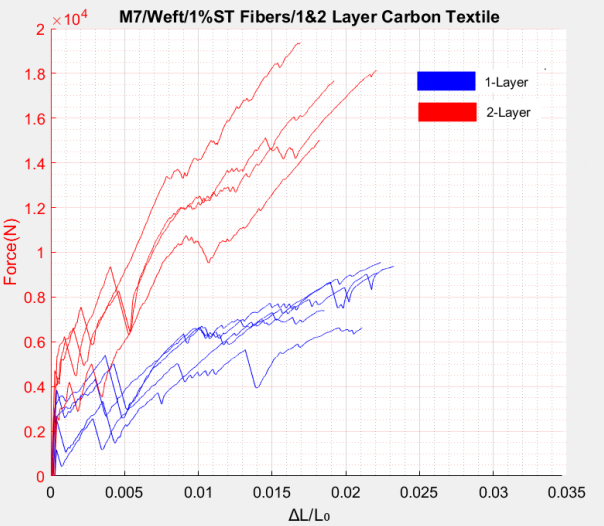

(b) 1% steel fibers

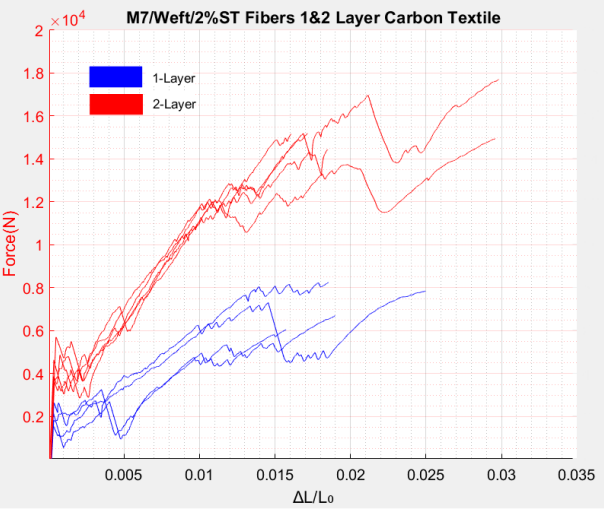

(c) 2% steel fibers

Figure 4-3 C-TRCC specimens with 1 and 2 layers of textile

As can be seen from that Figure 4-3, increasing the number of layers drastically increases the maximum tensile force that can be carried by the C-TRCC specimen. In order to better analyze the effects of steel fiber inclusion and the textile layers the data obtained from those figures is summarized as presented in Table 4-3.

Table 4-3 Tensile test results of C-TRCC specimens with the M7 Matrix

Mix ID	Steel Fiber Dosage	Textile Layers	Reinf. Ratio (ρ)	t	σ_{cr}	σ_u	Max $\Delta L/L_0$	F_{max}	Max. Stress on Textiles (σ_t)	Cracked Modulus of Elasticity (E_f)
	(%)		(%)	(mm)	(MPa)	(MPa)	(-)	(kN)	(MPa)	(MPa)
M7	0	1	0.44 [8]	12.2 [8]	2.7 [79]	6.9 [16]	0.012 [30]	8.3 [10]	1541 [10]	1297 [30]
		2	0.76 [9]	14.3 [9]	4.2 [9]	13.4 [13]	0.016 [28]	19.0 [8]	1759 [8]	1035 [28]
	1	1	0.49 [8]	11.1 [8]	3.8 [29]	9.0 [7]	0.012 [8]	10.0 [2]	1847 [2]	726 [11]
		2	0.71 [9]	15.4 [9]	4.3 [20]	13.1 [7]	0.019 [12]	19.83 [2]	1836 [2]	862 [16]
	2	1	0.48 [4]	11.3 [4]	3.0 [7]	8.5 [9]	0.019 [20]	9.20 [6]	1712 [6]	696 [15]
		2	0.75 [5]	14.5 [5]	4.0 [15]	12.4 [6]	0.022 [31]	19.10 [10]	1765 [10]	690 [25]

Due to the high variability (variability CoV thickness 81%, first cracking strength 79%) in 1 layer and 0% steel fiber incorporating specimens, DIC analysis was performed for all the specimens test set as shown in Figure 4-4. As shown in that figure, the specimens (#1, #2 and #5) with lower first cracking stresses experienced eccentricity (as identified by the diagonal crack pattern) while applying the uniaxial tensile load. This eccentricity could stem either from the test setup and/or the application of epoxy. Therefore, the values in that row are corrected as $\sigma_{cr} = 4.9$ MPa, $\sigma_u = 5.8$ MPa and E_f=1350 MPa which will be used in further analysis.

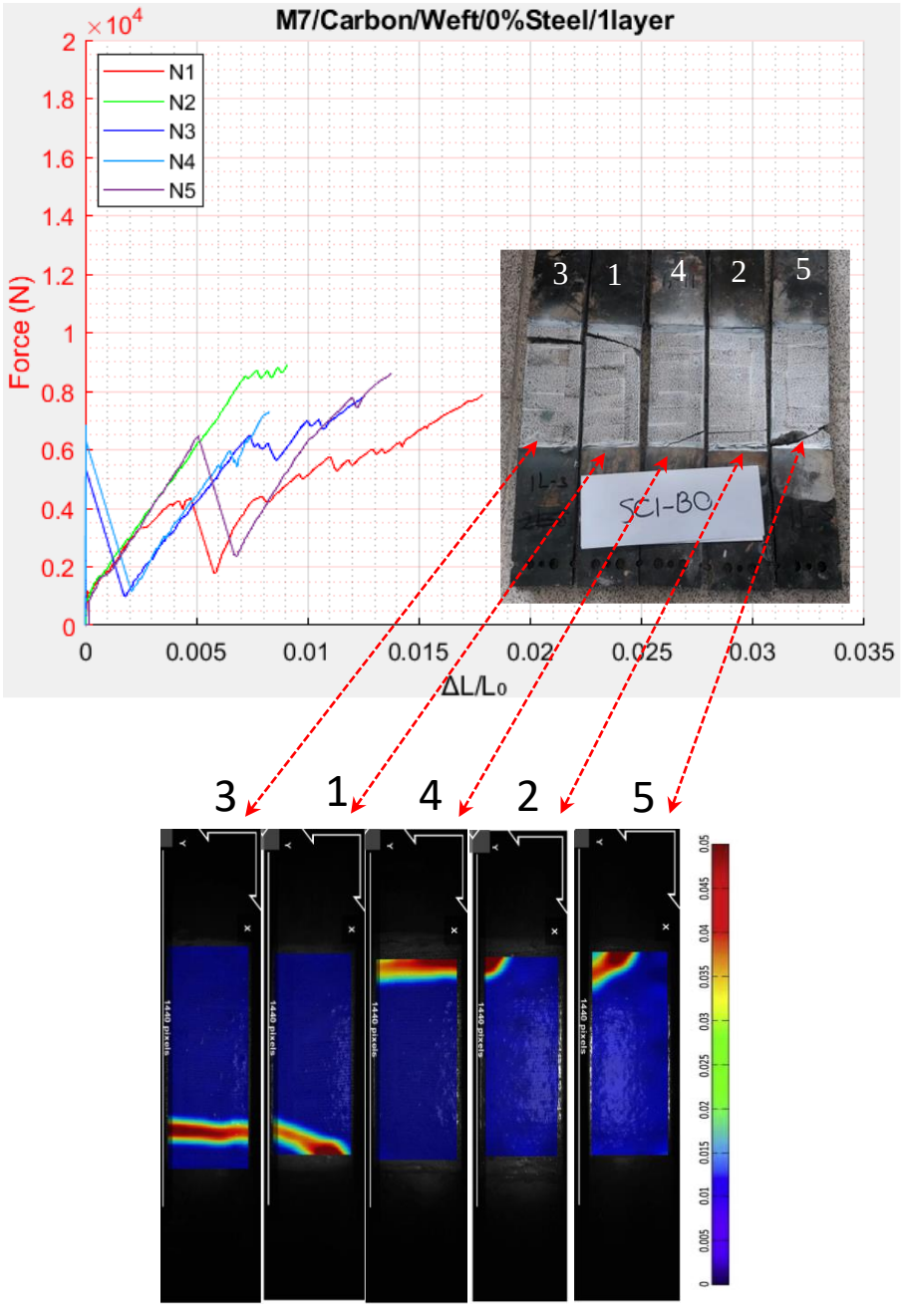

Figure 4-4 DIC analysis of specimens with 1 layer of textile and 0% steel fibers

As illustrated in Table 4-3, with the addition of short steel fibers (V_f=1%), first cracking strengths increased, however with additional steel fiber incorporation (V_f=1%) a slight reduction was observed. Moreover, textile reinforcement has a drastic effect on the ultimate strength of the composites (Textile Fibre &Civil Engineering, P.39).

On the other hand, as the textile layers increased, cracked elastic modulus also decreases. The reason could be due to the change in the failure mode of the specimens. In the one-layer specimens, textile rupture was the dominant failure mode, whereas in the two-layer specimens, the failure mode changed to textile slippage, and therefore the carbon textile deformations were much higher without as much change in ultimate strength, resulting in a reduction in the slope, i.e. E_f (Carozzi et al., 2017).

In addition, all C-TRCC samples with M7 matrix and ECC matrix without PVA fibers experienced spalling as shown in Figure 4-5. The reasons for this could be that the carbon textile has an elliptical shape in the weft direction, resulting in a larger surface area and therefore a tendency to slip, leading to spalling.

The other reason is that the modulus of elasticity of carbon fabric is higher than that of M7 and ECC matrices, so their deformation after stretching is different, causing relative slippage.

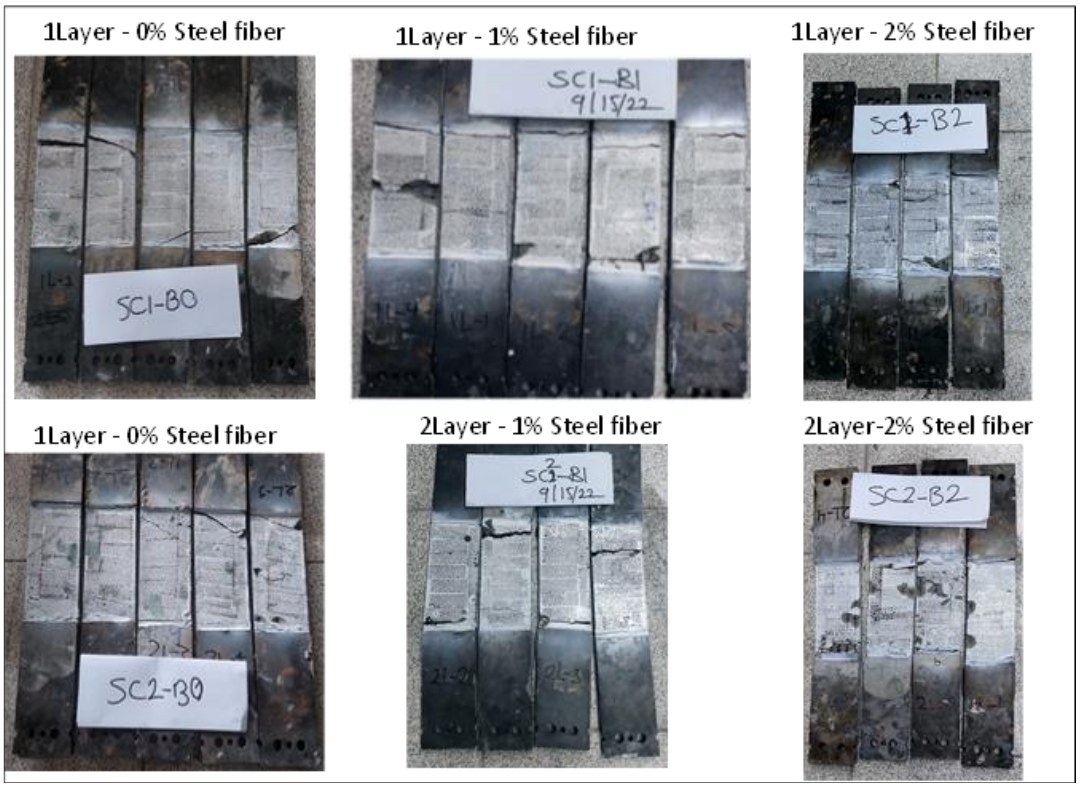

Figure 4-5 Spalling of M7 matrix specimens

4.4. Characterization of C-TRCC with the ECC matrix

The uniaxial compressive and tensile strength testing of the ECC matrix was initially performed and the results are presented in Table 4-4. Although the change in compressive strength with PVA fiber amount is not that obvious, the variation in the tensile strength was more noticeable.

Table 4-4 The characteristics of the ECC matrix in the absence of textiles

%PVA fibers by volume	**Compressive Strength (MPa)**		**Tensile Strength (MPa)**	
	Mean	**CoV (%)**	**Mean**	**CoV (%)**
0	57	5	0.9	30
1	66	6	1.7	26
2	57	7	3.4	23

In addition, when the load-normalized deformation plots are summarized in Table 4-5 provided in Appendix C is analyzed, it can be concluded that all ECC control specimens with no fibers exhibited a single crack leading to brittle failure. However, with 1 and 2% PVA fibers, strain-hardening behavior is observed and the ultimate strength increased, which is a typical ECC behavior.

Table 4-5 ECC Control Specimens, [] shows CoV

Mix ID	PVA Fiber Dosage	Thickness (t)	First Crack Strength (σ_{cr})	Ultimate Strength (σ_u)	$\Delta L/L_0$ at σ_u	max$\Delta L/L_0$	F_{max}
	(%)	(mm)	(MPa)	(MPa)	-	-	(kN)
ECC	0	15.7 [5]	0.62 [34]	0.62 [34]	0.000052 [34]	0.000052 [34]	0.9 [30]
	1	11.2 [4]	1.4 [20]	1.6 [19]	0.0007 [65]	0.0007 [65]	1.7 [26]
	2	14.4 [5]	2.2 [22]	2.6 [15]	0.0001 [57]	0.0003 [57]	3.4 [23]

After characterizing the ECC matrix, the mechanical properties of the C-TRCC specimens that had 1 and 2 layers of textiles were analyzed. Figure 4-6 presents the

results for 1 and 2 layers of textiles when the ECC matrix contain different amount of PVA fibers. As can be seen from that figure, increasing the number of layers of carbon textile increases the maximum tensile force that can be carried by the C-TRCC specimens. To better understand the effects of PVA fiber inclusion and the textile layers the data is summarized as presented in Table 4-6.

Table 4-6 Tensile test results of C-TRCC specimens with the ECC Matrix

Mix ID	Steel Fiber Dosage	Textile Layers	Reinf. Ratio (ρ)	t	σ_{cr}	σ_u	Max $\Delta L/L_0$	F_{max}	Max. Stress on Textiles (σ_t)	Cracked Modulus of Elasticity (E_f)
	(%)		(%)	(mm)	(MPa)	(MPa)	(-)	(kN)	(MPa)	(MPa)
M7	0	1	0.50 [13]	10.4 [8]	3.9 [29]	7.5 [21]	0.009 [16]	8.4 [6]	1547 [6]	1138 [12]
		2	0.96 [5]	13.7 [6]	3.5 [25]	13.2 [21]	0.014 [37]	17.8 [16]	1647 [16]	893 [21]
	1	1	0.49 [10]	11.2 [7]	3.5 [22]	8.4 [10]	0.022 [45]	9.7 [7]	1805 [7]	797 [73]
		2	0.67 [4]	15.1 [5]	2.8 [39]	11.0 [8]	0.026 [5]	17.9 [11]	1654 [11]	521 [6]
	2	1	0.38 [10]	14.3 [6]	3.9 [9]	6.8 [12]	0.022 [53]	9.6 [7]	1782 [7]	880 [42]
		2	0.57 [7]	18.9 [4]	3.7 [11]	8.1 [5]	0.020 [32]	15.3 [7]	1418 [7]	674 [26]

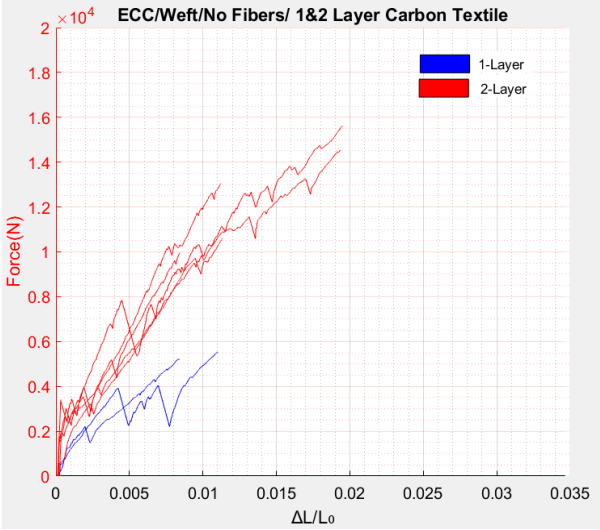

(a) No PVA fibers

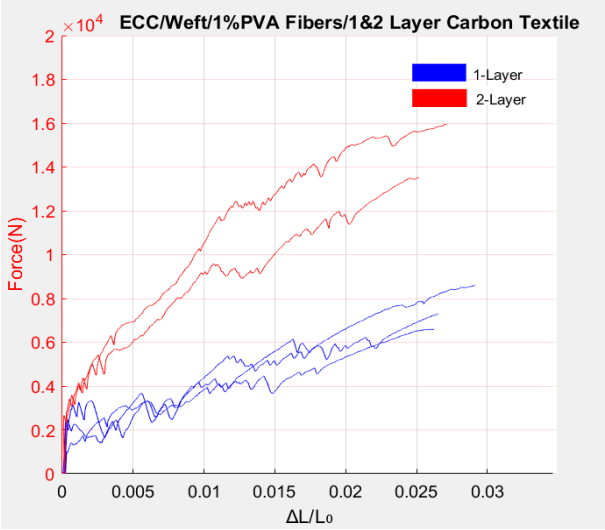

(b) 1% PVA fibers

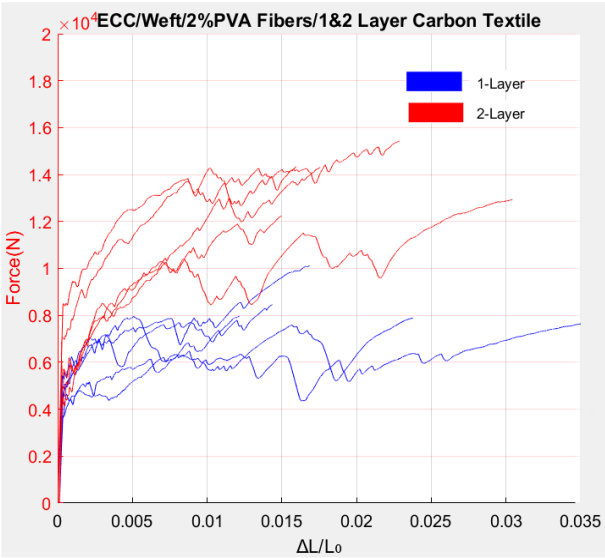

(c) 2% PVA fibers

Figure 4-6 C-TRCC specimens with 1 and 2 layers of textile

As the textile layers increased, the ultimate strength increased as illustrated in Figure 4-6. On the other hand, when the 2-layer textiles were used there was a reduction in the ultimate strength with increasing PVA fiber volume. It should be mentioned that as the PVA fibers could not pass through the grids of the textile, the manufacturing technique was changed to laminating technique which increased the specimen thicknesses. Therefore, the thicker matrix per layer will increase the Young's modulus of the composite, but it will affect the short fiber bridging mechanism and decreasing the cracked modulus and ultimate strength (Li et al., 2019). For instance, 1418 MPa elastic cracked modulus for 2 layer textile 2% fibers could be due to slippage, reduction in ultimate forces resulting in lower stress on textile. Moreover, while applying uniaxial load, the textile experienced slippage that could be another reason for this reduction in the ultimate strength of C-TRCC specimens with 2-layer textiles.

On the other hand, it should be noted that when the matrix was changed to ECC, spalling was only observed in the absence of PVA fibers, in other words, the use of PVA fibers at 1% and 2% eliminated spalling in the C-TRCC specimens as illustrated in Figure 4-7. The reason for the spalling was already explained during the M7 matrix sub-section.

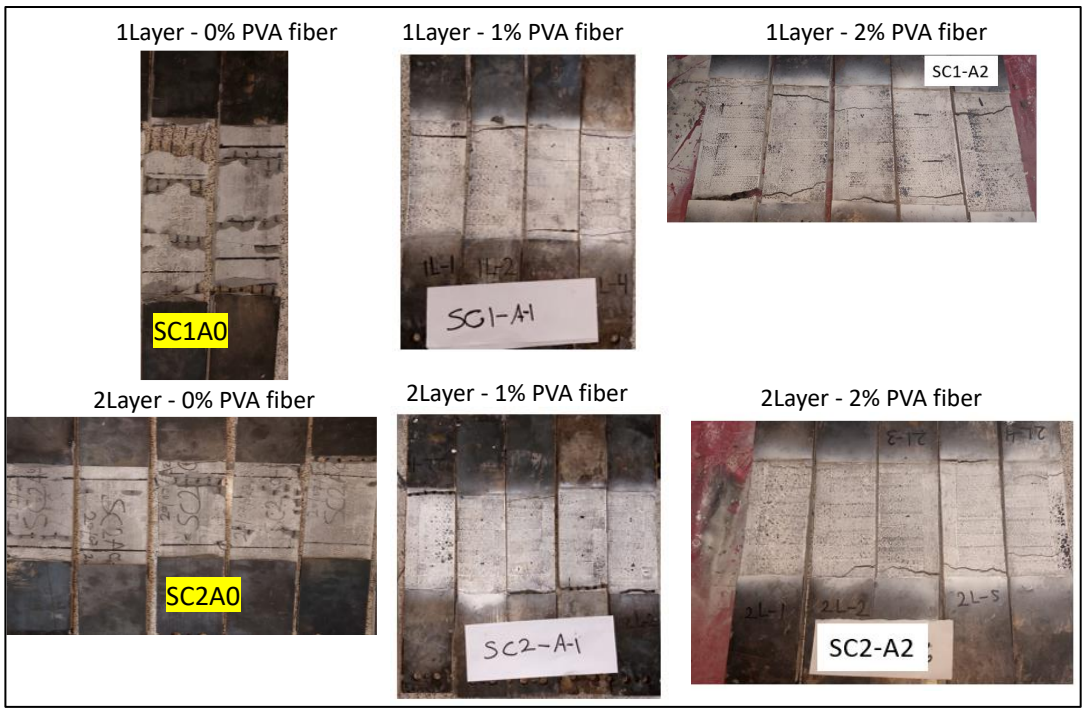

Figure 4-7 Spalling of ECC matrix specimens

On the other hand, due to the usage of low reinforcement ratio for the ECC matrix, all C-TRCC specimens experienced between 1 and 3 cracks as shown in Appendix C. By increasing the layers of textiles, more cracks were noticed as shown in Figure 4-8.

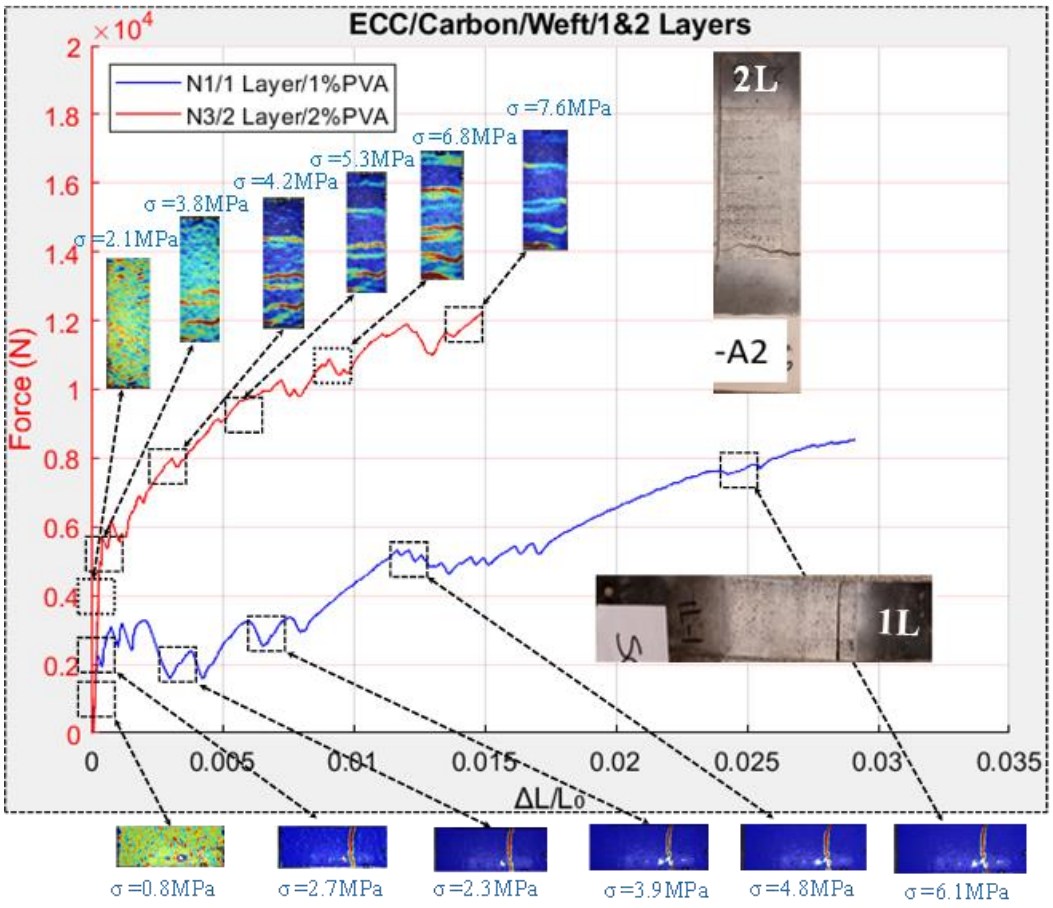

Figure 4-8 DIC of 1 &2 layer of ECC specimens

Commonly, for C-TRCC specimens, the effect of PVA fibers after the first crack is negligible because the textile is dominant one that takes the uniaxial load. Similar observations on the Ef could also be made for the ECC mixtures.

4.5. Comparison of the M7 and the ECC matrices

In this section, a comparative evaluation of both matrices is made in terms of the short fiber volume incorporated in the C-TRCC specimens, as well as the number of textile layers, for the different parameters obtained and summarized previously. Line plots are provided to see the influence of the use of short fibers and the carbon textile layers.

4.5.1 The cracking strength

From the data plotted in Figure 4-9, it can be clearly seen that an increase in first crack was observed with the addition of fibers in the absence of textile. However, the use of fibers together with the textile not only complicated the detection of the first crack but also the casting procedure therefore no meaningful explanations could be made.

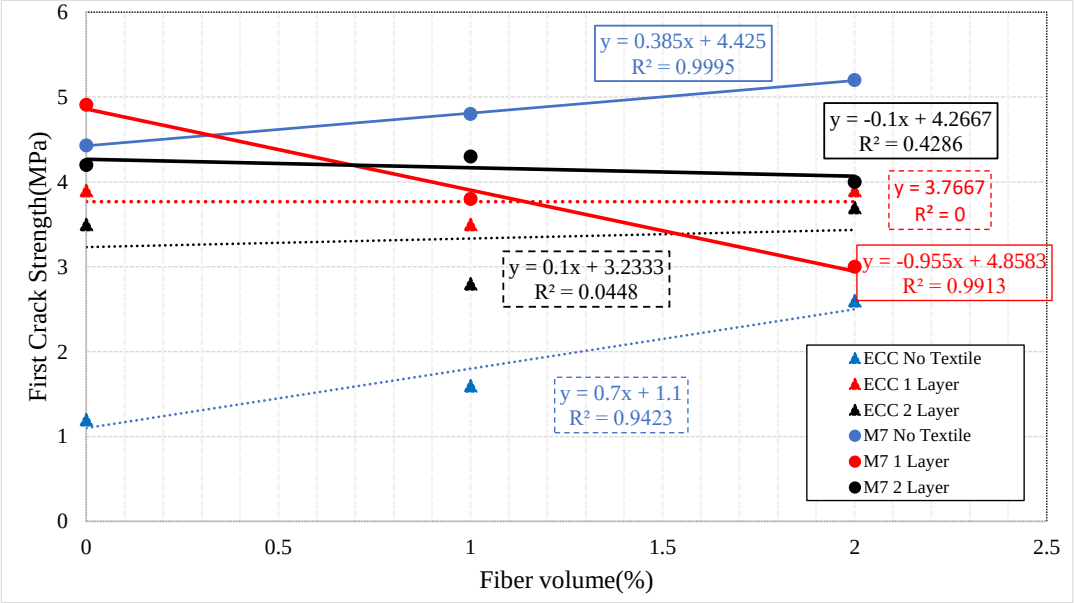

Figure 4-9 First Cracking Strength of C-TRCC specimens with ECC and M7 matrices

4.5.2 The normalized deformation

By comparing the normalized deformation of C-TRCC for both matrices as shown in Figure 4-10, it can be inferred that the use of textiles brings ductility. Moreover, ECC mixtures on average seem to have a slightly better ductility then the M7 mixtures.

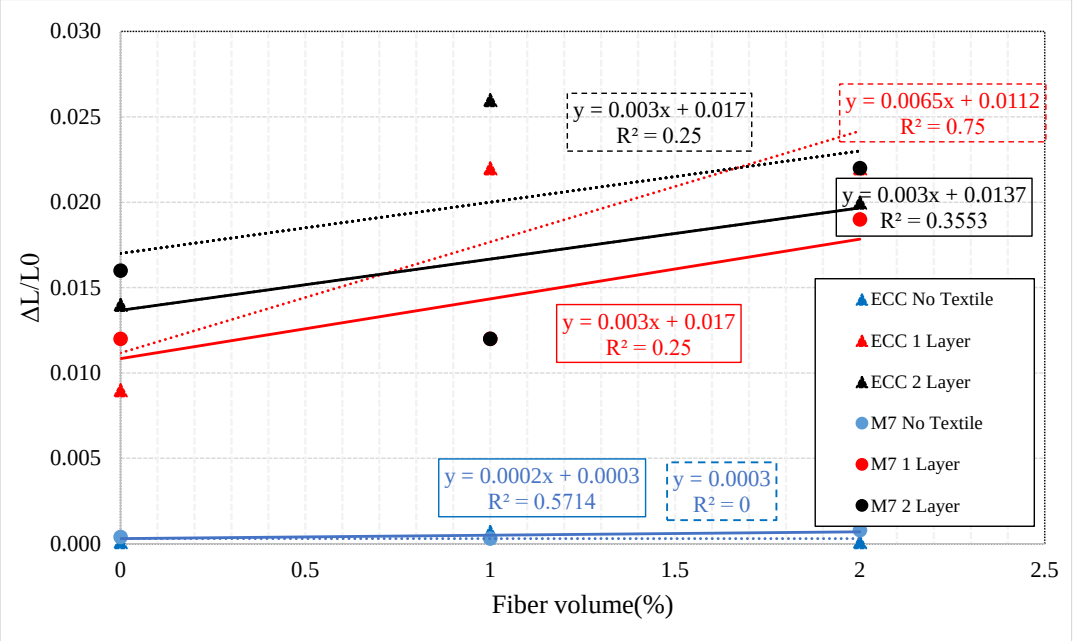

Figure 4-10 Normalized deformation of C-TRCC specimens with ECC and M7 matrices

4.5.3 The cracked modulus of elasticity

The cracked modulus of elasticity, E_f, after initial slope is calculated using the ACI434 formula as explained previously. In general, as shown in Figure 4-11, E_f seems to reduce with both textile incorporation as well as short fiber inclusion.

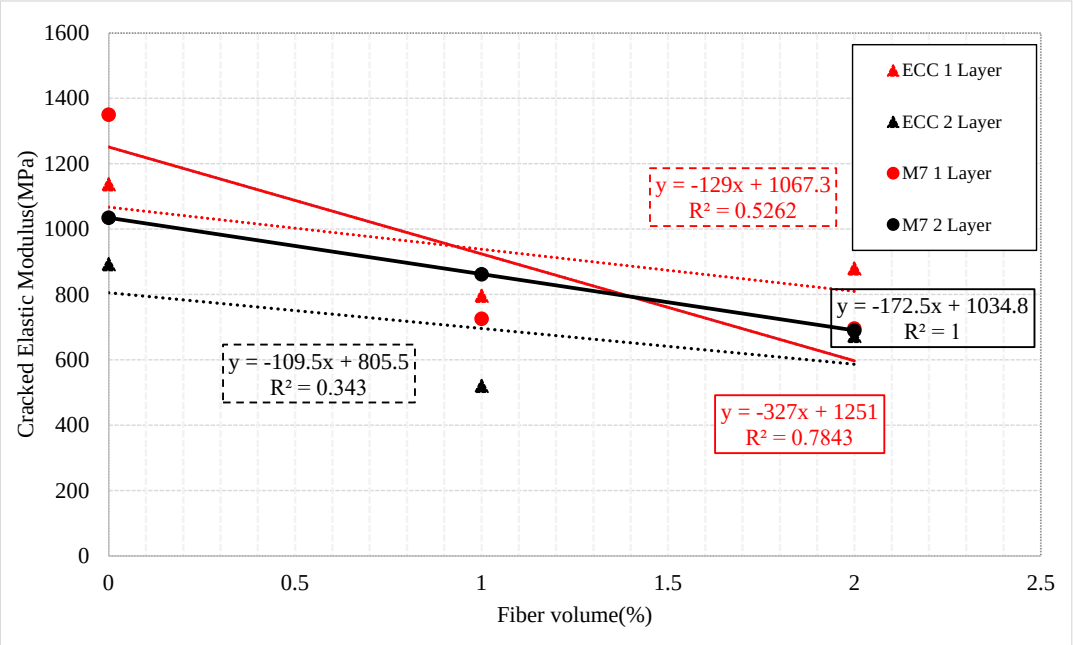

Figure 4-11 Cracked Elastic Modulus of C-TRCC specimens with ECC and M7 matrices

4.5.4 Ultimate strength

As observed from Figure 4-12, in the absence of textiles, the M7 matrix has a higher strength than the ECC matrix, and for both matrices, increasing the amount of short fibers increased their ultimate strength. Moreover, for both matrices, the carbon textile reinforcement increased the ultimate strength of the composite. However, when the textiles are used in combination with the short fibers, their interaction causes some difficulties in interpreting the results. As mentioned earlier, it was difficult to cast the specimens during the specimen preparation due to the poor workability of the mixtures especially with the high volume of short fibers (V_f=2%). This was more evident for the two-layer textile incorporating specimens, where both ECC and M7 mixtures show a reduction in the ultimate strength, with ECC showing a steeper decline than M7.

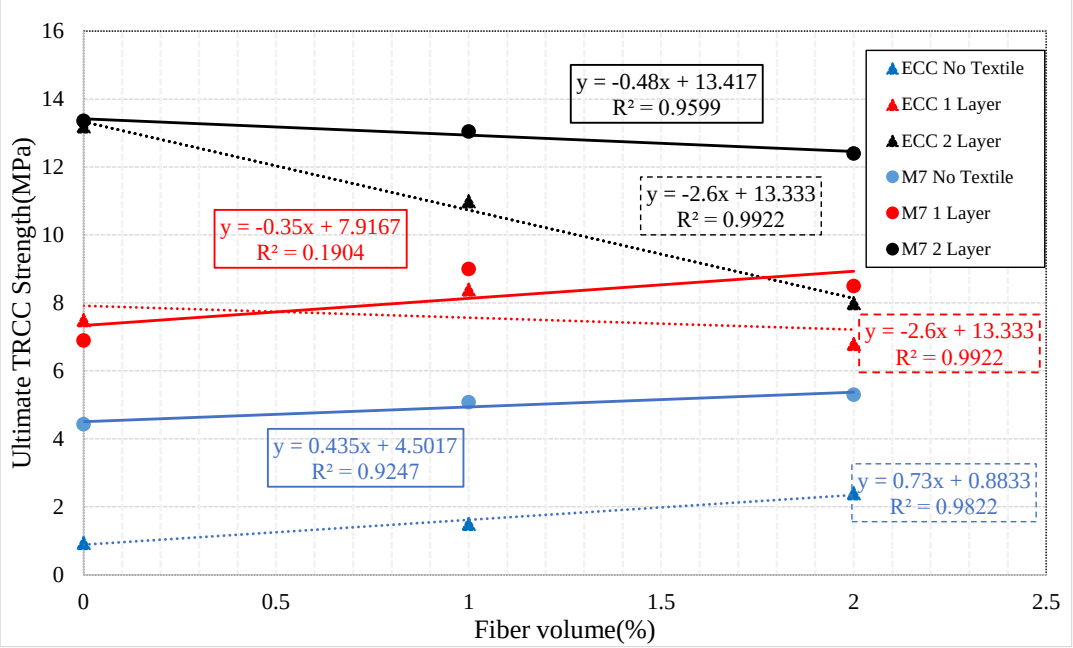

Figure 4-12 Ultimate strength of C-TRCC specimens with ECC and M7 matrices

4.5.5 Energy absorption capacity

The energy absorption capacities were determined from the area under the C-TRCC stress and normalized deformation curves, and are presented in Figure 4-13. In general, the energy absorption capacities increased with the addition of short fibers as well as with an increased in the number of textile layers. Due to their higher ultimate strengths, the M7 mixtures exhibited a higher energy absorption capacity compared to the ECC mixtures. On average when compared to the ECC mixtures, the increase in energy absorption capacity was 11% for 1 layer and 25% for 2 layer M7 mixtures.

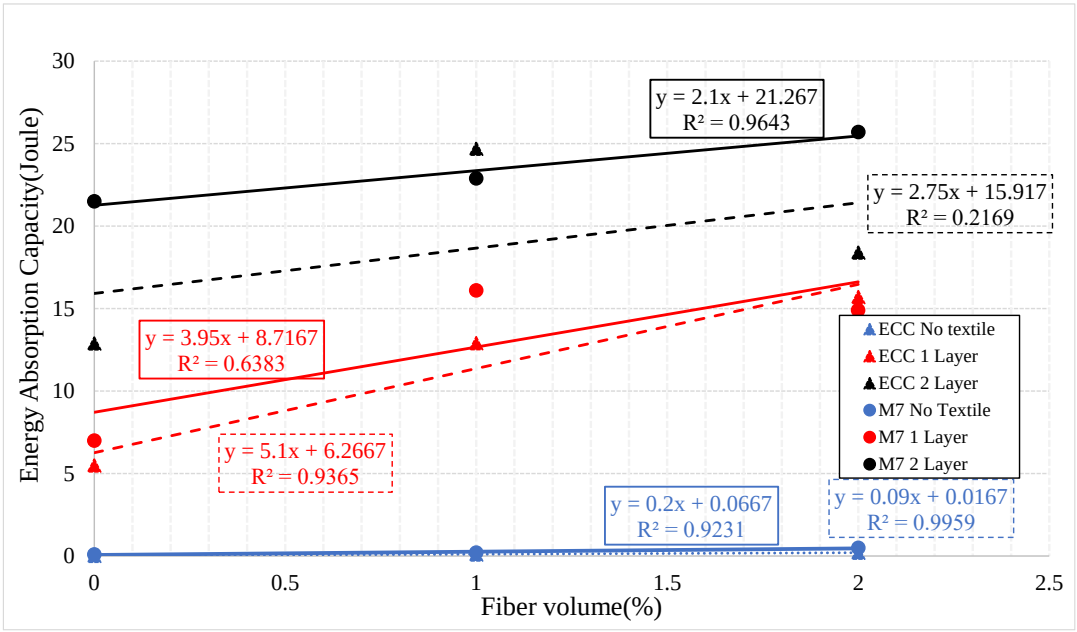

Figure 4-13: Energy absorption capacity of C-TRCC specimens with ECC and M7 matrices

CHAPTER 5

CONCLUSIONS AND RECOMMENDATIONS

In this experimental investigation the effect of carbon textile in the weft direction and fiber dosage content was thoroughly investigated using two types of matrices. The load-normalized deformations curves and energy absorption capacities were determined. When necessary, digital image correlations were also carried out using N_{corr} software to characterize the crack patterns.

- By increasing the amount of short fibers, especially PVA fibers, a significant reduction in the workability of the compounds was observed. Even though, the use of chemical admixtures provided a better workability, the casting of ECC blends incorporating 2% fibers was only possible by using a laminated composite manufacturing process.
- Due to the high stiffness of the carbon textile and the high surface area of the textile in the weft direction, spalling occurred in all C-TRCC specimens using the M7 matrix, and the incorporation of the short steel fibers was not able to eliminate the spalling. On the other hand, for the softer ECC matrix, although spalling was also observed in the absence of short PVA fibers, the incorporation of the PVA fibers eliminated the spalling.
- Increasing the reinforcement ratio of the textile increased both the uniaxial tensile load and the deformation capacity, regardless of the matrix composition. On the other hand, the effect of short fibers on the uniaxial tensile behavior of C-TRCC specimens is quite complex and also involves the specimen preparation stage. By increasing the amount of PVA fibers in the ECC mixtures, the ultimate strength of C-TRCC specimens decreased substantially due to reduced workability. Therefore, the amount of short fiber volume should be optimized depending on the reinforcement ratio.
- It was also observed that the uniaxial behavior of C-TRCC specimens can be improved by the addition of a suitable matrix with short discrete fibers. The

use of short discrete fibers resulted in an increase in crack number and strain hardening behavior. As a result, a significant increase in the area under the stress-strain curves and a high energy absorption capacity were obtained. On average, the increase in energy absorption capacity was 11% for 1 layer and 25% for 2 layer M7 blends compared to ECC blends.

The following recommendations are made for future researchers planning on working in this area:

- For steel plates used in the clevis type of loading, it is advisable to apply the uniaxial load from a single point. This is because by applying the force at a single point, eccentricity can also be minimized to avoid eccentric moment in TRC specimens.
- The cracked modulus of elasticity seems to decrease with both textile and short fiber inclusion, and further investigation is needed to understand why.
- Modeling and analytical studies are necessary to understand the behavior of textiles in cementitious composites.
- As the ECC mixtures contained a high amount of fly ash, their behavior in the long term should also be studied.

REFERENCES

Abid, M. S., & Rathod, D. (2022). Bearing Capacity of Asphalt-Coated Jute Textile Reinforced Sand. *Geotechnical and Geological Engineering*, *40*(7), 3457–3475. https://doi.org/10.1007/s10706-022-02106-9

Ahmad, J., Zaid, O., Aslam, F., Martínez-García, R., Elharthi, Y. M., Hechmi EI Ouni, M., Tufail, F., & Sharaky, I. A. (2021). Mechanical properties and durability assessment of nylon fiber reinforced self-compacting concrete. *Journal of Engineered Fibers and Fabrics*, *16*. https://doi.org/10.1177/15589250211062833

Alma, M., & Ghiassi, B. (2021). *applied sciences Durability of Textile Reinforced Concrete : Existing Knowledge and Current Gaps*.

Andrade, F. De, Butler, M., Mechtcherine, V., Zhu, D., & Mobasher, B. (2011). *Strain rate effect on the tensile behaviour of textile-reinforced concrete under static and dynamic loading*. *528*, 1727–1734. https://doi.org/10.1016/j.msea.2010.11.014

Aydinç Güzelce(2019).Effect of fiber type and concrete strength on the energy absorption capacity of fiber reinforced concrete plates under quasi-static bending[MSc-Master Program thesis], Middle East Technical University.

Barhum, R., & Mechtcherine, V. (2010). Effect of short fibres on fracture behaviour of textile reinforced concrete. *Fracture Mechanics of Concrete and Concrete Structures, 2004*, 1498–1503. http://framcos.org/FraMCoS-7/12-17.pdf

Batson, G. (1976). Steel fiber reinforced concrete. *Materials Science and Engineering*, *25*(C), 53–58. https://doi.org/10.1016/0025-5416(76)90051-3

Brückner, A., Ortlepp, R., & Curbach, M. (2006). Textile reinforced concrete for strengthening in bending and shear. *Materials and Structures/Materiaux et Constructions*, *39*(8), 741–748. https://doi.org/10.1617/s11527-005-9027-2

Carozzi, F. G., Bellini, A., D'Antino, T., de Felice, G., Focacci, F., Hojdys, Ł., Laghi, L., Lanoye, E., Micelli, F., Panizza, M., & Poggi, C. (2017). Experimental investigation of tensile and bond properties of Carbon-FRCM composites for strengthening masonry elements. *Composites Part B: Engineering*, *128*, 100–119. https://doi.org/10.1016/j.compositesb.2017.06.018

Cibulka, T., Musil, L., & Vodička, J. (2019). The lightweight textile reinforced concrete for thin-walled structures. *Acta Polytechnica CTU Proceedings*, *22*, 17–21. https://doi.org/10.14311/APP.2019.22.0017

Contamine, R., Larbi, A. S., & Hamelin, P. (2011). Contribution to direct tensile testing of textile reinforced concrete (TRC) composites. *Materials Science & Engineering A*, *528*(29–30), 8589–8598. https://doi.org/10.1016/j.msea.2011.08.009

Das, C. S., Dey, T., Dandapat, R., Mukharjee, B. B., & Kumar, J. (2018). Performance evaluation of polypropylene fibre reinforced recycled aggregate concrete. *Construction and Building Materials*, *189*, 649–659. https://doi.org/10.1016/j.conbuildmat.2018.09.036

De Santis, S., Hadad, H. A., De Caso y Basalo, F., de Felice, G., & Nanni, A. (2018). Acceptance Criteria for Tensile Characterization of Fabric-Reinforced Cementitious Matrix Systems for Concrete and Masonry Repair. *Journal of Composites for Construction*, *22*(6), 1–14. https://doi.org/10.1061/(asce)cc.1943-5614.0000886

Deng, M., Dong, Z., & Zhang, C. (2020). Experimental investigation on tensile behavior of carbon textile reinforced mortar (TRM) added with short polyvinyl alcohol (PVA) fibers. *Construction and Building Materials*, *235*, 117801. https://doi.org/10.1016/j.conbuildmat.2019.117801

Dong, Z., Deng, M., Zhang, C., Zhang, Y., & Sun, H. (2020). Tensile behavior of glass textile reinforced mortar (TRM) added with short PVA fibers. *Construction and Building Materials*, *260*, 119897.

https://doi.org/10.1016/j.conbuildmat.2020.119897

Du, Y., Zhang, M., Zhou, F., & Zhu, D. (2017). Experimental study on basalt textile reinforced concrete under uniaxial tensile loading. *Construction and Building Materials*, *138*, 88–100. https://doi.org/10.1016/j.conbuildmat.2017.01.083

Esmaeili, J., Sharifi, I., Andalibi, K., & Kasaei, J. (2017). Effect of Different Matrix Compositions and Micro Steel Fibers on Tensile Behavior of Textile Reinforced Concrete. *IOP Conference Series: Materials Science and Engineering*, *246*(1). https://doi.org/10.1088/1757-899X/246/1/012031

Traintafillou, Thanasis C.(2016).Textile Fiber Composite in Civil Engineering, Elsevier Inc., doi: 10.1016/C2014-0-01415-3, ISBN: 9781782424697

Giorgia, I., Anna, C., Zani, G., & Colombo, M. (2013). *Erratum to : Textile Reinforced Concrete : experimental investigation on design parameters*. 1953–1971. https://doi.org/10.1617/s11527-013-0023-7

Hartig, J., Häußler-Combe, U., & Schicktanz, K. (2008). Influence of bond properties on the tensile behaviour of Textile Reinforced Concrete. *Cement and Concrete Composites*, *30*(10), 898–906. https://doi.org/10.1016/j.cemconcomp.2008.08.004

Heins, K., Lesker, S., Pütz, J., Hüntemann, M., & Gries, T. (2023a). Effect of thermoplastic impregnation on the mechaHeins, K., Lesker, S., Pütz, J., Hüntemann, M., & Gries, T. (2023). Effect of thermoplastic impregnation on the mechanical behaviour of textile reinforcement for concrete. SN Applied Sciences, 5(3). https:/. *SN Applied Sciences*, *5*(3). https://doi.org/10.1007/s42452-023-05305-y

Heins, K., Lesker, S., Pütz, J., Hüntemann, M., & Gries, T. (2023b). Effect of thermoplastic impregnation on the mechanical behaviour of textile reinforcement for concrete. *SN Applied Sciences*, *5*(3). https://doi.org/10.1007/s42452-023-05305-y

Heravi, A. A., Fuchs, A., Gong, T., Curosu, I., Kaliske, M., & Mechtcherine, V. (2020). Mechanical characterization of textile reinforced cementitious composites under impact tensile loading using the split Hopkinson tension bar. *Cement and Concrete Composites*, *114*(January), 103769. https://doi.org/10.1016/j.cemconcomp.2020.103769

Holčapek, O., Vogel, F., & Reiterman, P. (2017). Using of Textile Reinforced Concrete Wrapping for Strengthening of Masonry Columns with Modified Cross-section Shape. *Procedia Engineering*, *195*, 62–66. https://doi.org/10.1016/j.proeng.2017.04.524

Jesse, D., & Jesse, F. (2009). Tragverhalten von Textilbeton unter zweiaxialer Zugbeanspruchung *. *4th Colloquium on Textile Reinforced Structures (CTRS4)*, *January 2009*, 129–144.

Keskin, S. B. (2012). *Dimensional Stability of Engineered Cementitious Composites*. *September*, 165. http://etd.lib.metu.edu.tr/upload/12614713/index.pdf

Lee, J. H., Cho, B., Choi, E., & Kim, Y. H. (2016). Experimental study of the reinforcement effect of macro-type high strength polypropylene on the flexural capacity of concrete. *Construction and Building Materials*, *126*, 967–975. https://doi.org/10.1016/j.conbuildmat.2016.09.017

Li, B., Xiong, H., Jiang, J., & Dou, X. (2019). Tensile behavior of basalt textile grid reinforced Engineering Cementitious Composite. *Composites Part B: Engineering*, *156*(July 2018), 185–200. https://doi.org/10.1016/j.compositesb.2018.08.059

Lieboldt, M., & Mechtcherine, V. (2013). Capillary transport of water through textile-reinforced concrete applied in repairing and/or strengthening cracked RC structures. *Cement and Concrete Research*, *52*, 53–62. https://doi.org/10.1016/j.cemconres.2013.05.012

Liu, D., Huang, H., Yue, Q., Xue, Y., & Wang, M. (2016). Behaviour of tunnel lining strengthened by textile-reinforced concrete. *Structure and Infrastructure Engineering*, *12*(8), 964–976. https://doi.org/10.1080/15732479.2015.1076009

Mansur de Castro Silva, R., & de Andrade Silva, F. (2020). Carbon textile reinforced concrete: materials and structural analysis. *Materials and Structures/Materiaux et Constructions*, *53*(1). https://doi.org/10.1617/s11527-020-1448-4

Mechtcherine, V. (2013). Novel cement-based composites for the strengthening and repair of concrete structures. *Construction and Building Materials*, *41*, 365–373. https://doi.org/10.1016/j.conbuildmat.2012.11.117

Mechtcherine, V. (2016). Durability of structures made of or strengthened using textile-reinforced concrete. *Textile Fibre Composites in Civil Engineering*, 151–168. https://doi.org/10.1016/B978-1-78242-446-8.00007-0

Naaman, A. E. (2010). Textile Reinforced Cement Composites: Competitive status and research directions. *International RILEM Conference on Material Science*, *I*, 3–22.

Peled, A., Mobasher, B., & Bentur, A. (2017). Textile reinforced concrete. In *Textile Reinforced Concrete*. https://doi.org/10.1201/9781315119151

Portal, N. W., Lundgren, K., Wallbaum, ; Holger, Malaga, K., & Asce, A. M. (2014). Sustainable Potential of Textile-Reinforced Concrete. *Journal of Materials in Civil Engineering*, *27*(7), 04014207. https://doi.org/10.1061/(ASCE)MT.1943-5533.0001160

Chao, C. T. R. C. A., Wu, C., Pan, Y., & Yan, L. (2023). *Mechanical Properties and Durability of Textile Reinforced. Polymers 2023, 15,3826.https:doi.org/10.3390/polym1583826*.

RILEM Technical Committee 232-TDT (Wolfgang Brameshuber), Brameshuber, W., Hinzen, M., Dubey, A., Peled, A., Mobasher, B., Bentur, A., Aldea, C.,

Silva, F., Hegger, J., Gries, T., Wastiels, J., Malaga, K., Papanicolaou, C., Taerwe, L., Curbach, M., Mechtcherine, V., Naaman, A., Orlowsky, J., … Jesse, F. (2016). Uniaxial tensile test: test method to determine the load bearing behavior of tensile specimens made of textile reinforced concrete. *Materials and Structures/Materiaux et Constructions*, *49*(12), 4923–4927. https://doi.org/10.1617/s11527-016-0839-z

Şahmaran, M., Lachemi, M., Hossain, K. M. A., & Li, V. C. (2009). Internal curing of engineered cementitious composites for prevention of early age autogenous shrinkage cracking. *Cement and Concrete Research*, *39*(10), 893–901. https://doi.org/10.1016/j.cemconres.2009.07.006

Saidi, M., Reboul, N., & Gabor, A. (2022). Analysis of bond behaviour of textile-reinforced cement (TRC) applied to masonry using distributed fibre optic sensors and acoustic emission. *Composites Part B: Engineering*, *247*(September). https://doi.org/10.1016/j.compositesb.2022.110327

Santis, S. De, Giulia, F., Felice, G. De, & Poggi, C. (2017). Test methods for Textile Reinforced Mortar systems. *Composites Part B*, *127*, 121–132. https://doi.org/10.1016/j.compositesb.2017.03.016

Sengun, E., Sherzai, M. H., Mercan, A. M., Guzelce, A., Alam, B., & Yaman, I. O. (2023). The impact of specimen size and alteration of fiber configuration on the flexural performance of high-performance concrete. *Journal of Building Engineering*, *68*(December 2022), 106142. https://doi.org/10.1016/j.jobe.2023.106142

Spencer, D. J. (1989). *Knitting Technology*.A Comprehensive Handbook and Practical Guide, Elsevier, Apr 27,201. ISBN:9781855737556

Tiedemann, E. J., & Jakes, K. A. (2006). An exploration of prehistoric spinning technology: Spinning efficiency and technology transition. *Archaeometry*, *48*(2), 293–307. https://doi.org/10.1111/j.1475-4754.2006.00257.x

Triantafillou, T. C. (2016). Textile Fibre Composites in Civil Engineering. In

Textile Fibre Composites in Civil Engineering. Elsevier Inc. https://doi.org/10.1016/C2014-0-01415-3

Valeri, P., Fernàndez Ruiz, M., & Muttoni, A. (2020). Tensile response of textile reinforced concrete. *Construction and Building Materials*, *258*, 119517. https://doi.org/10.1016/j.conbuildmat.2020.119517

Venigalla, S. G., Nabilah, A. B., Nasir, N. A. M., Safiee, N. A., & Abd Aziz, F. N. A. (2022). Textile-Reinforced Concrete as a Structural Member: A Review. *Buildings*, *12*(4). https://doi.org/10.3390/buildings12040474

Weber, W. E., & Mechtcherine, V. (2016). Modeling the dynamic properties of fibre-reinforced concrete with different coating technologies of multifilament yarns. *Cement and Concrete Composites*, *73*, 257–266. https://doi.org/10.1016/j.cemconcomp.2016.07.017

Williams Portal, N., Lundgren, K., Wallbaum, H., & Malaga, K. (2015). Sustainable Potential of Textile-Reinforced Concrete. *Journal of Materials in Civil Engineering*, *27*(7). https://doi.org/10.1061/(asce)mt.1943-5533.0001160

Williams Portal, N., Nyholm Thrane, L., & Lundgren, K. (2017). Flexural behaviour of textile reinforced concrete composites: experimental and numerical evaluation. *Materials and Structures/Materiaux et Constructions*, *50*(1), 1–14. https://doi.org/10.1617/s11527-016-0882-9

Yang, J. M., Lee, J., & Chang, C. (2023). Effect of Reinforcement Ratio and Bond Characteristic on Flexural Behavior of Carbon Textile-Reinforced Concrete Panels. *Materials*, *16*(10). https://doi.org/10.3390/ma16103703

Yao, Y., Bonakdar, A., Faber, J., Gries, T., & Mobasher, B. (2016). Distributed cracking mechanisms in textile-reinforced concrete under high speed tensile tests. *Materials and Structures/Materiaux et Constructions*, *49*(7), 2781–2798. https://doi.org/10.1617/s11527-015-0685-4

Zhang, P., Wei, S., Wu, J., Zhang, Y., & Zheng, Y. (2022). Investigation of mechanical properties of PVA fiber-reinforced cementitious composites under

the coupling effect of wet-thermal and chloride salt environment. *Case Studies in Construction Materials*, *17*(July), e01325. https://doi.org/10.1016/j.cscm.2022.e01325

Zhu, D., Liu, S., Yao, Y., Li, G., Du, Y., & Shi, C. (2019). Effects of short fiber and pre-tension on the tensile behavior of basalt textile reinforced concrete. *Cement and Concrete Composites*, *96*(January 2018), 33–45. https://doi.org/10.1016/j.cemconcomp.2018.11.015

APPENDIX – A: TERMINOLOGY OF TRC

The following terminology is summarized from the following documents

- ASTM 3878-07 Standard Terminology for Composite Materials
- ASTM D123-13a Standard Terminology Relating to Textiles

Bundle	a general term for a collection of essentially parallel filaments
Fabric	refers to a planar textile
Filament	A fiber of indefinite length
Mesh	in coated carbon yarn, the number of warp yarns or ends per linear 25.4mm followed by the number of filling yarns or picks per linear 25.4mm
Monofilament	a yarn consisting of one filament only
Roving	in fibrous composites, large filaments count tow
Sizing	an agent, normally resin, added to yarn to keep fibers in a non-twisted yarn together and/or to improve adhesion to the matrix in composites
Strand	in fibrous composite, synonym for tow
Textile	A general term applied to fibers and organized assemblies of fibers with sufficient integrity to maintain the organization
Tow	an essentially twist free assemblage of a large number of substantially parallel filaments
Thread	is a long, light strand composed of materials such as cotton, nylon, or other fibers commonly employed for sewing purposes
Tex	it refers to the unit of measurement for the linear weight of textile materials. It can be defined as the mass in grams of 1000 meters of a yarn. For instance, a tex of 30 means that 1000 meters of yarn weigh 30 grams

Warp	The machine direction for a weaving machine/yarn across the width of the fabric
Weft	The direction across the width of a weaving machine/yarns across the width of a fabric
Yarn	a continuous, ordered assembly of substantially parallel, collimated filaments, normally with twist, may consist of either discontinuous or continuous filaments

APPENDIX-B: FORCE-DEFORMATION PLOTS OF M7 MIXTURES

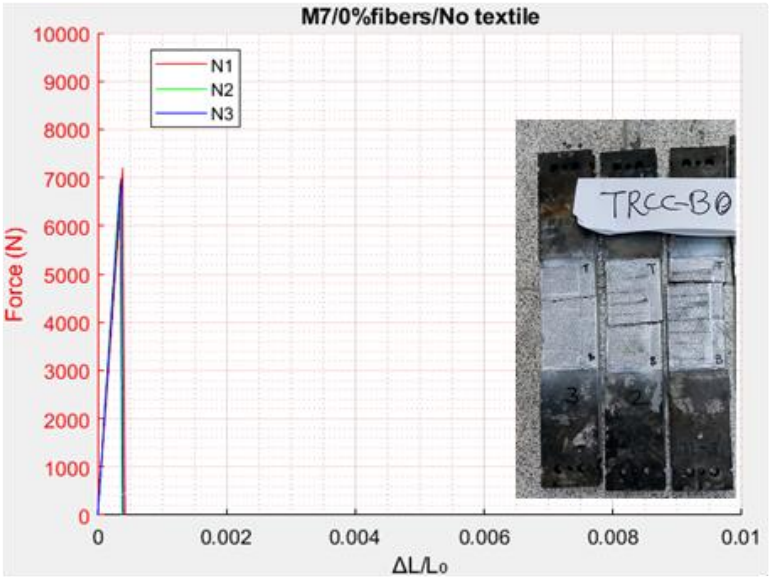

Figure B-1 M7 Control no fibers

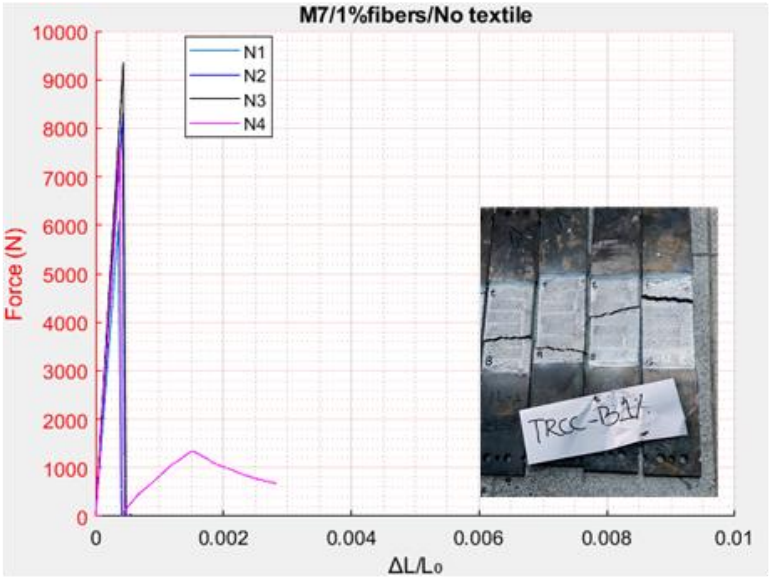

Figure B-2 M7 Control 1%fibers

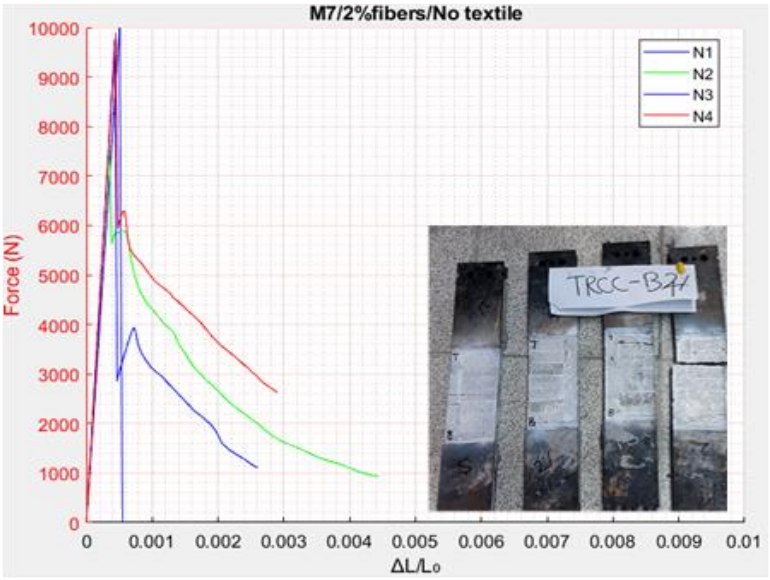

Figure B-3 M7 control 2%fibers

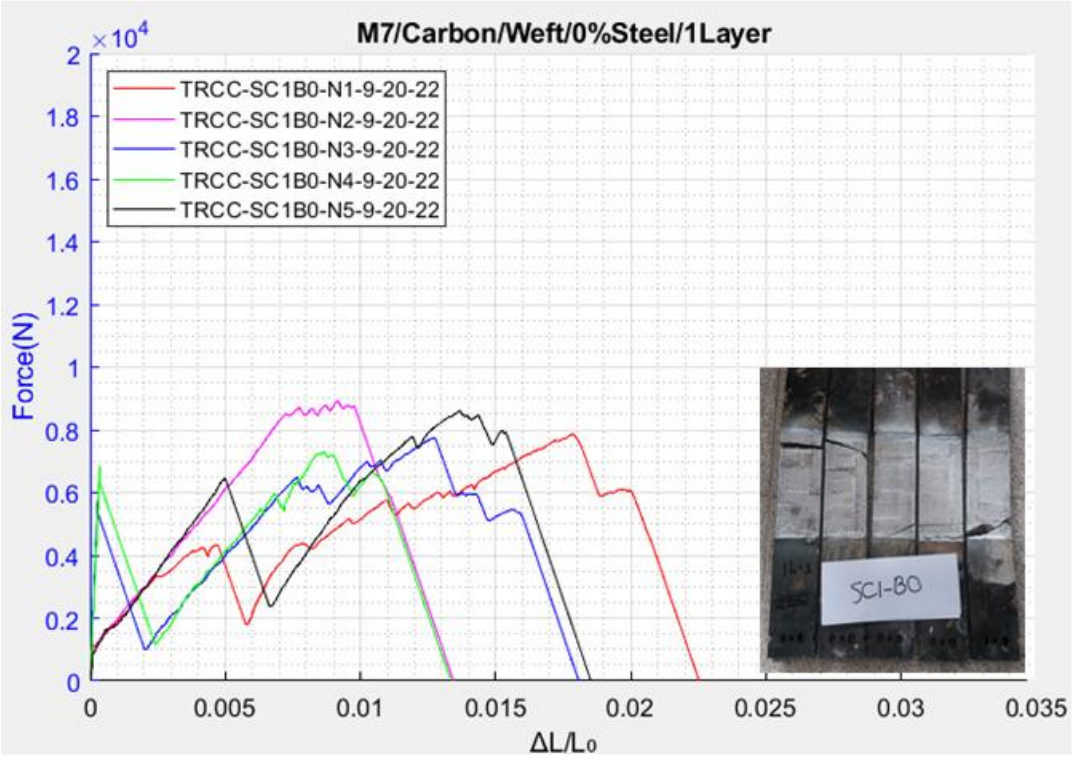

Figure B-4 No fibers 1 layer of carbon textile

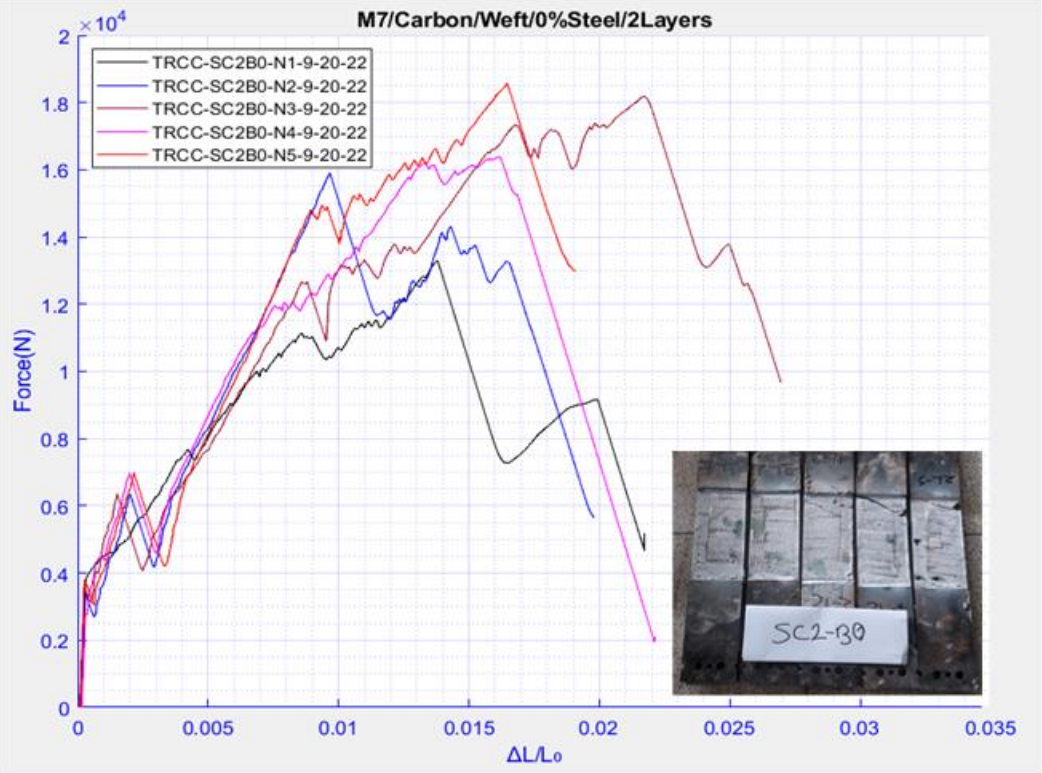

Figure B-5 No fibers 2 layer of carbon textile

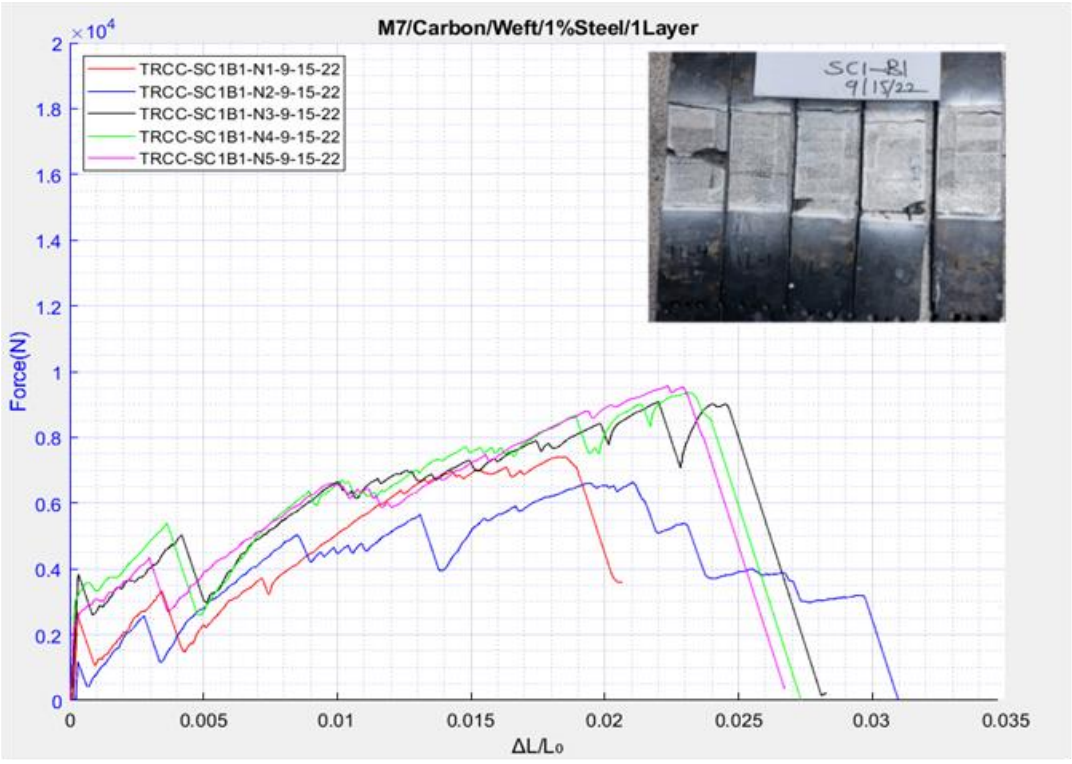

Figure B-6 1% fibers 1 layer of carbon textile

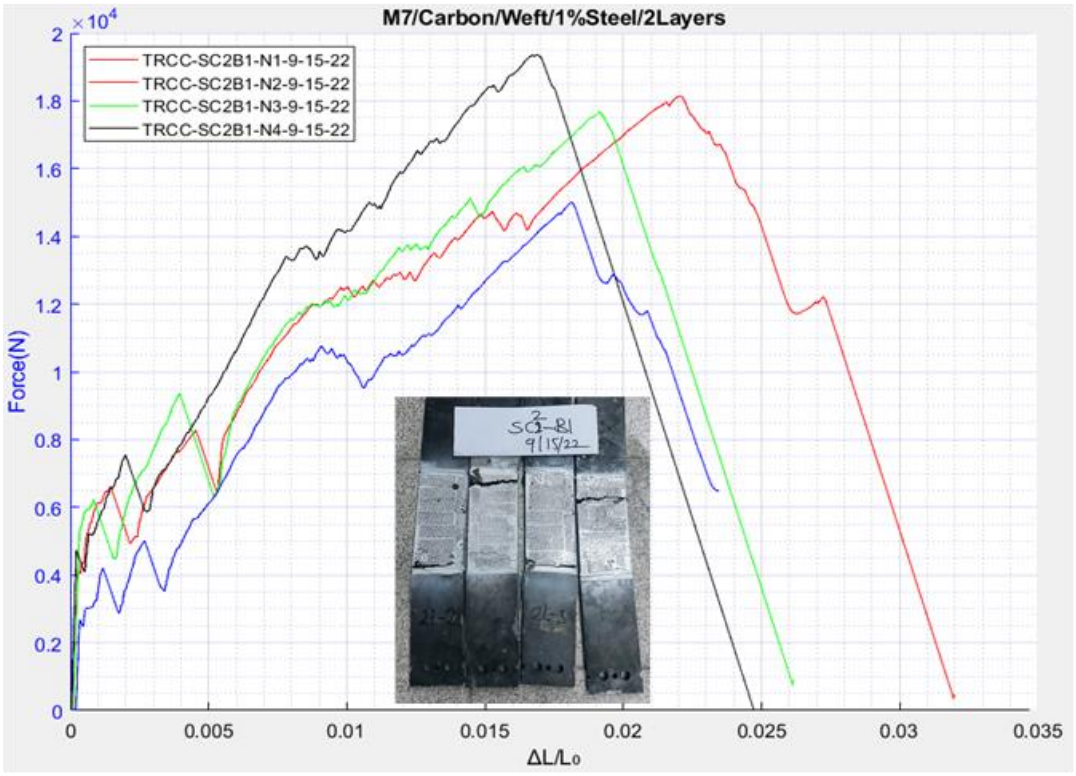

Figure B- 1% fibers 2 layer of carbon textile

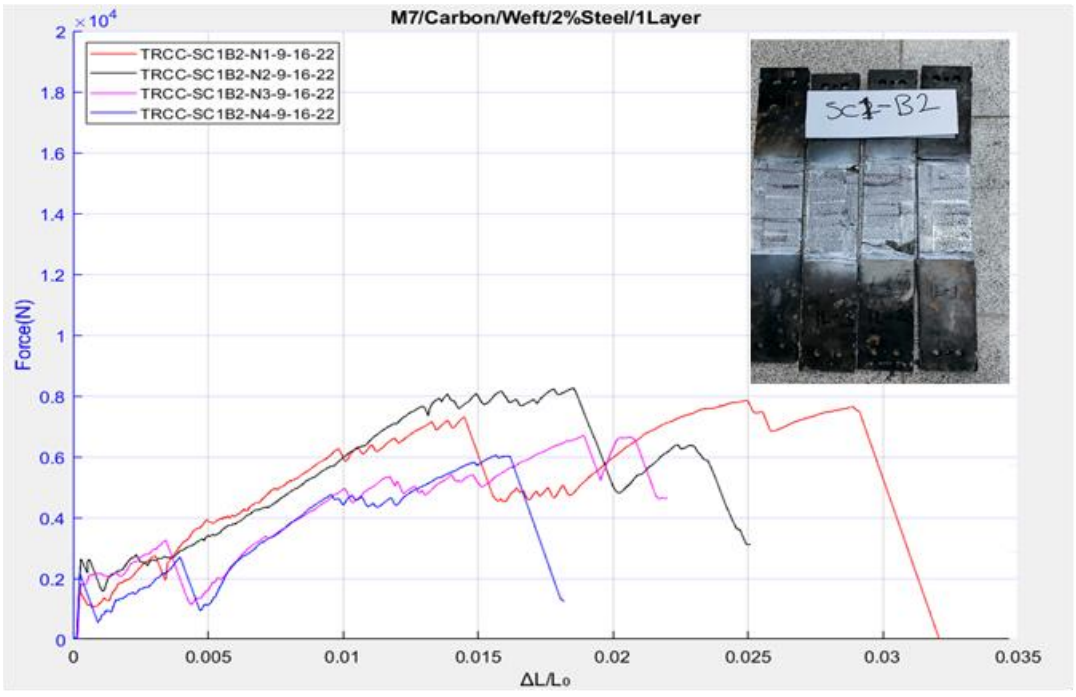

Figure B-7 2% fibers 1 layer of carbon textile

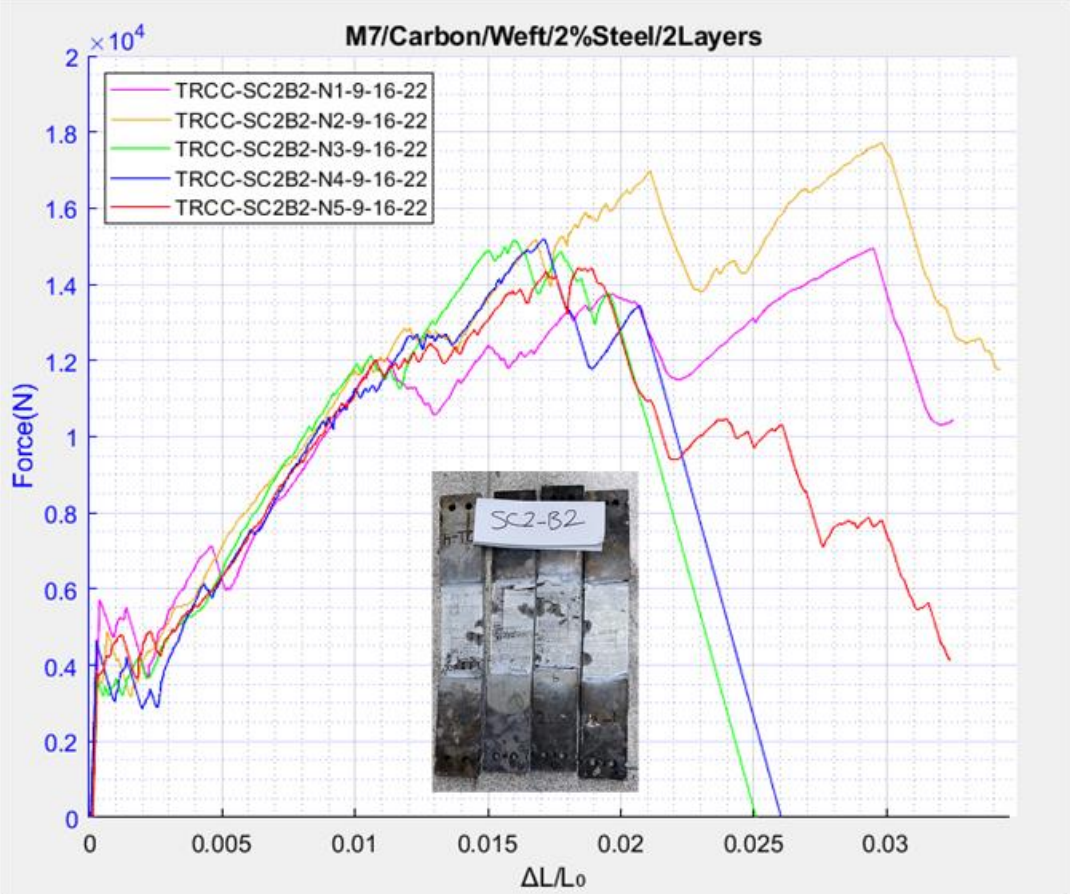

Figure B-8 2% fibers 2 layer of carbon textile

APPENDIX – C: FORCE-DEFORMATION PLOTS OF ECC MIXTURES

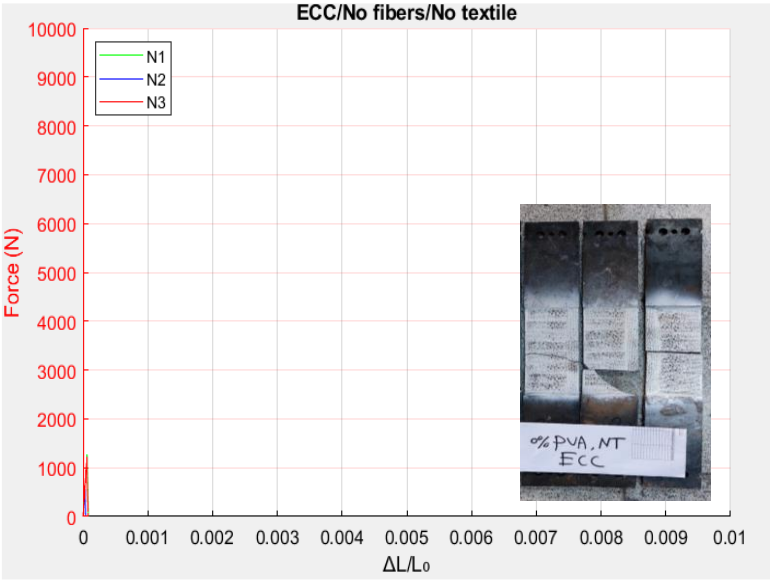

Figure C-1 ECC Control no fibers

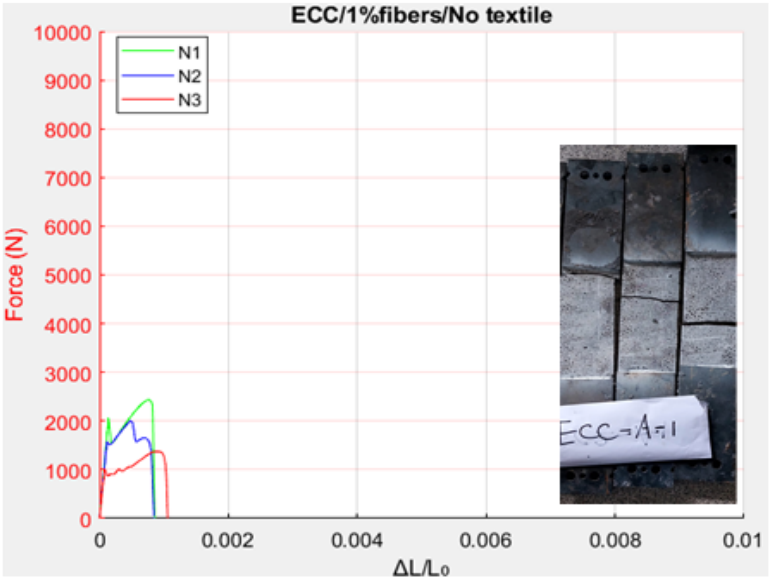

Figure C-2 ECC Control 1%PVA

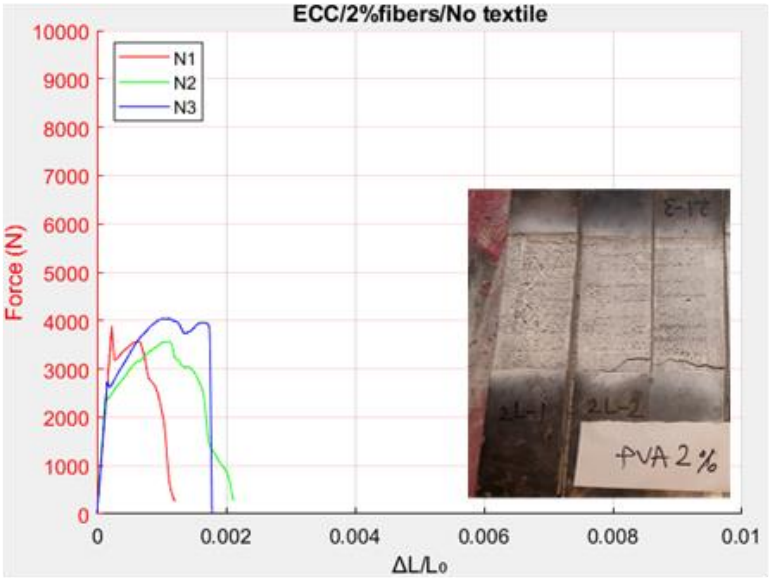

Figure C-3 ECC Control 2%PVA

Figure C-4 No fibers 1 layer of carbon textile

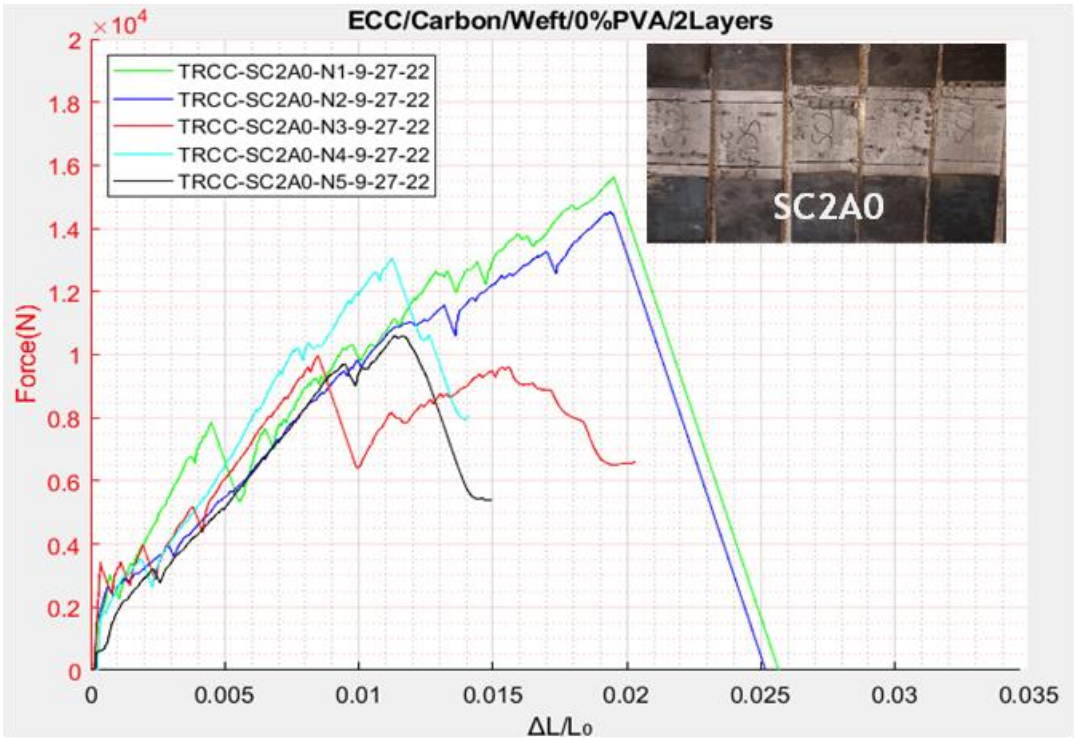

Figure C-5 No fibers 2 layer of carbon textile

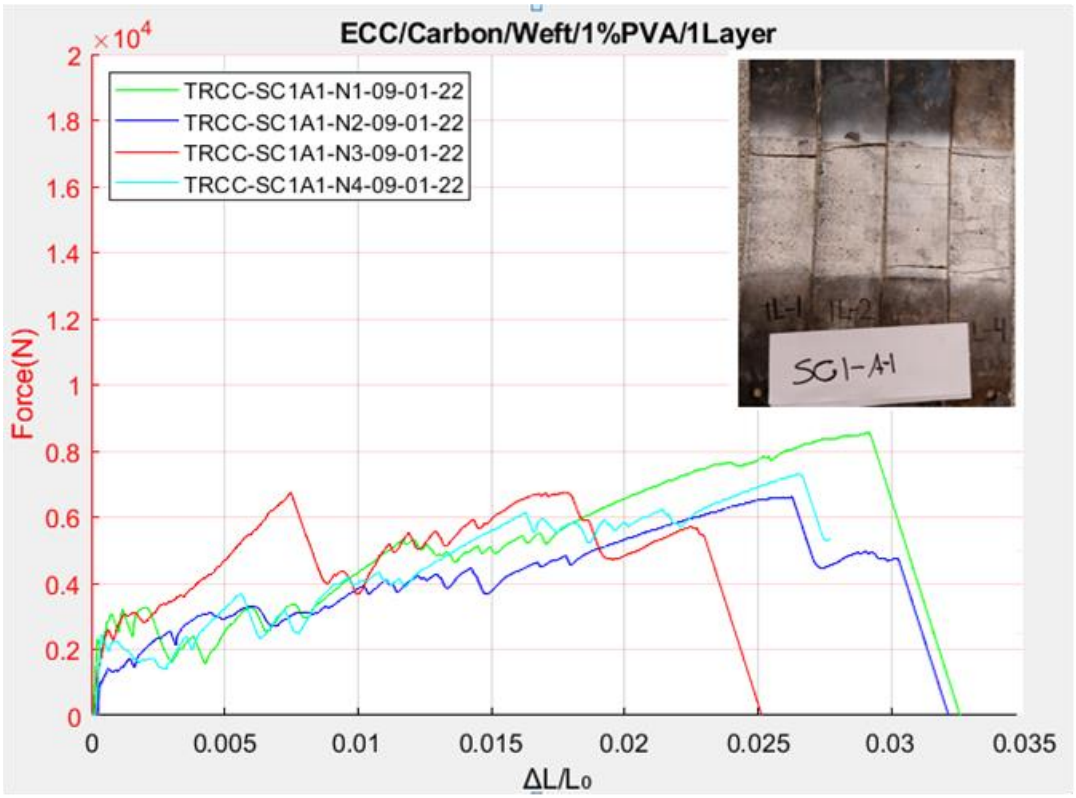

Figure C-6 1% fibers 1 layer of carbon textile

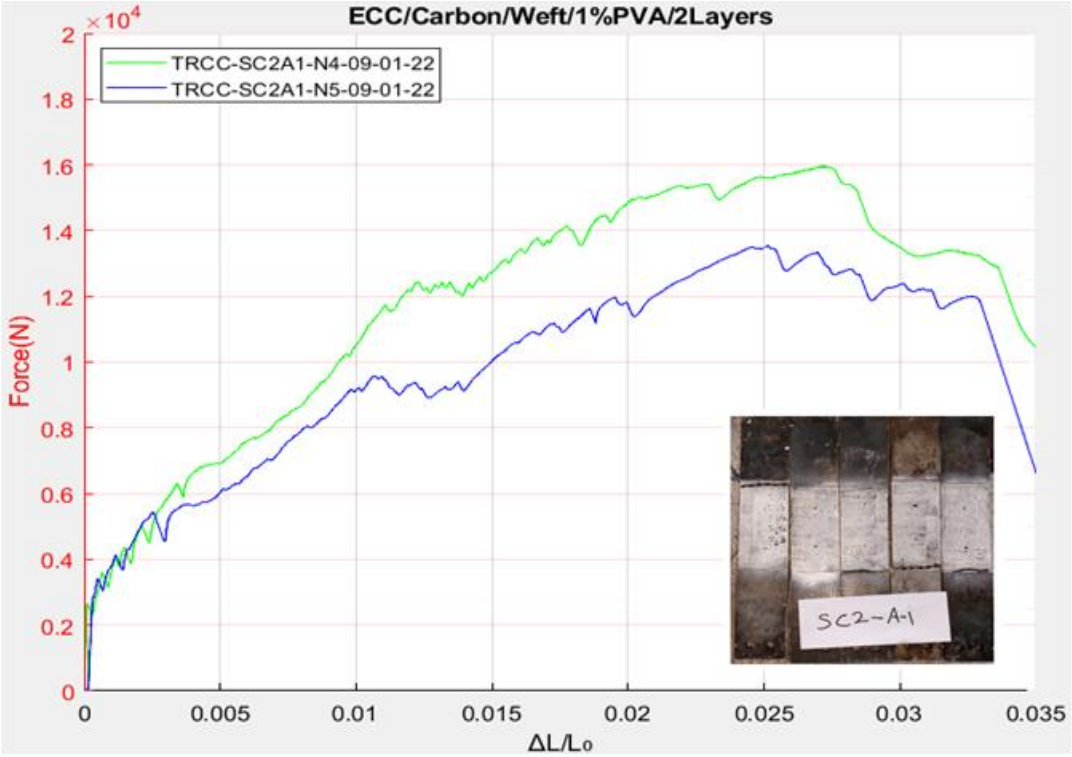

Figure C-7 1% fibers 2 layer of carbon textile

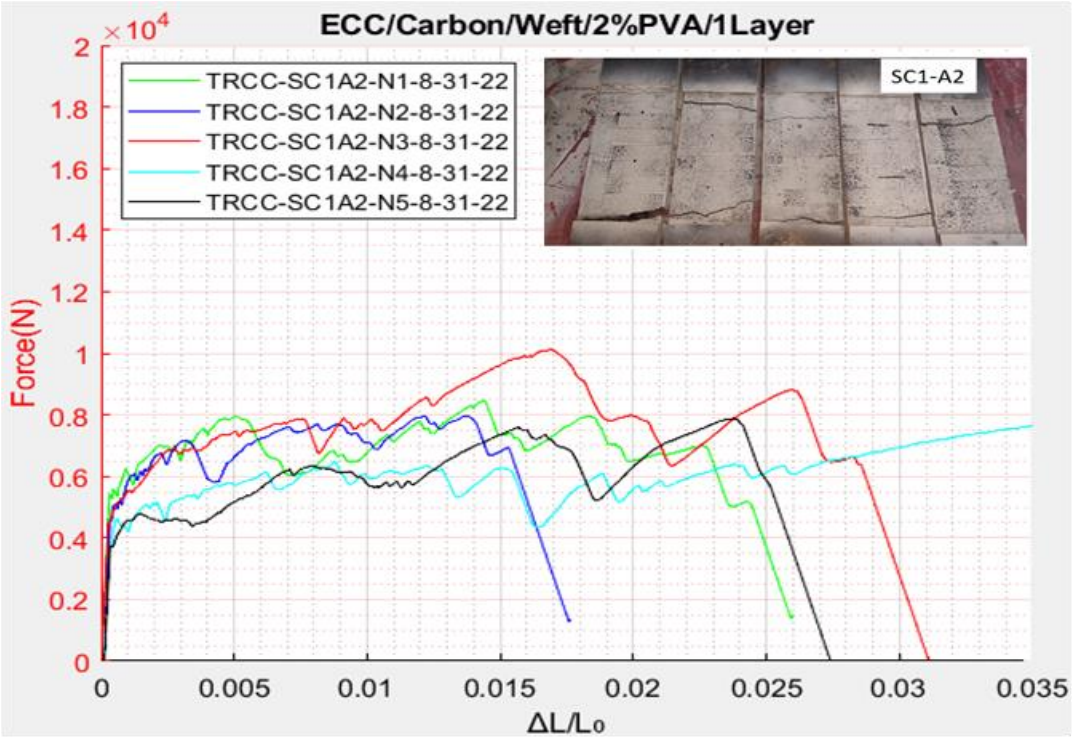

Figure C-8 2% fibers 1 layer of carbon textile

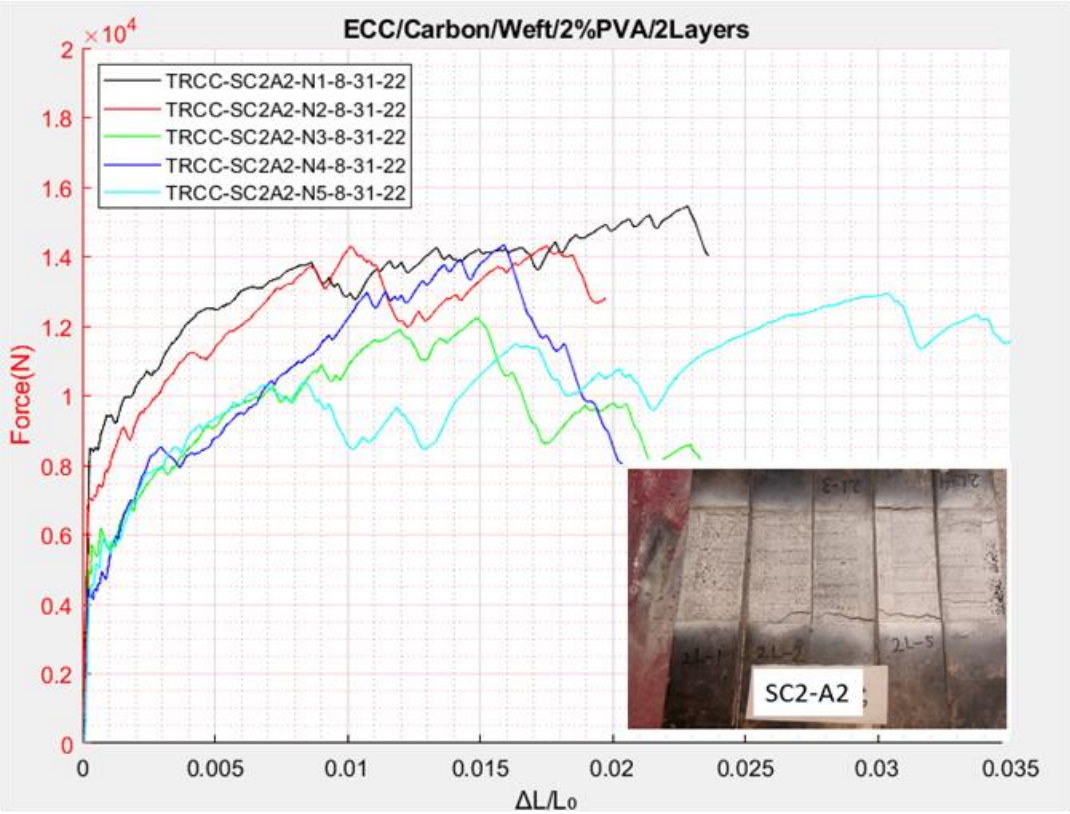

Figure C-9 2% fibers 2 layer of carbon textile